Modelling of soil degradation and its impact on ecosystem services globally

Part 1: A study on the adequacy of models to quantify soil water erosion for use within the IMAGE modeling framework

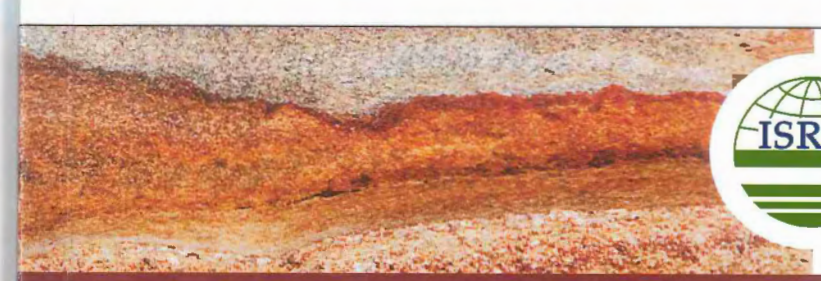

ISRIC World Soil Information

ISRIC Report 2013/06

S. Mantel, C.J.E. Schulp and M. van den Berg

PBL Netherlands Environmental Assessment Agency

Modelling of soil degradation and its impact on ecosystem services globally

Part 1: A study on the adequacy of models to quantify soil water erosion for use within the IMAGE modeling framework

S. Mantel (ISRIC), C.J.E. Schulp(PBL, now Free University of Amsterdam), M. van den Berg (PBL, now JRC)

ISRIC – World Soil Information, Wageningen, The Netherlands

PBL - Netherlands Environmental Assessment Agency, Bilthoven

ISRIC Report 2013/06

Wageningen, 2014

PBL Netherlands Environmental Assessment Agency

ISN: 2308569

Director, ISRIC – World Soil Information
PO BOX 353
6700 AJ Wageningen
The Netherlands
E-mail: soil.isric@wur.nl

Additional information on ISRIC – World Soil Information can be accessed through http://www.isric.org

Citation
Mantel, S. (ISRIC), C.J.E. Schulp (PBL, now Free University of Amsterdam), M. van den Berg (PBL, now JRC) *Modelling of soil degradation and its impact on ecosystem services globally, Part 1: A study on the adequacy of models to quantify soil water erosion for use within the IMAGE modeling framework* Report 2014/xx, ISRIC—World Soil Information, Wageningen.
74 pages,28 figures and 12 tables.

Photo cover: Istock

ISRIC Report 2013/06

Contents

Preface

The mandate of ISRIC – World Soil Information is to collect, increase and disseminate, worldwide knowledge of the land, its soils in particular, and to support their sustainable use and management. Mapping land degradation and assessment of its impact on functions of land and soil has been a focal activity of ISRIC over the years.

This study is a further elaboration, towards implementation of modelling at the global scale, of the studies done by ISRIC at National level on quantification of the impact of soil erosion on crop production for the United Nations Environment Programme (UNEP) in collaboration with the National Institute of Public Health and Environment (PBL) of the Netherlands, that were published between 1997 and 2001. It links with other ISRIC studies done in collaboration with PBL and other, international, partners. In this report methods are explored for quantification of soil quality decline in modelled scenarios of socio-economic or environmental changes. It focusses on methods for quantification of the soil erosion by water, its projected impact on soil properties and on crop production at broad scales (1 and 10 km resolution of elevation data). A review and evaluation of regional to global soil erosion models was made first. Subsequently, and two models were tested for consistency of their output at two data resolutions. A possible pathway for implementation of the method, integrating more quantified modelling of soil erosion in the global modelling framework of IMAGE, Integrated Model to Assess the Global Environment, is provided.

Improved quantification of land degradation and its impact on land functions, among which productivity and water conservation, will contribute to a better understanding of human impact on the environment and may contribute to formulation of possible pathways towards a more sustainable society.

Dr. ir. Hein van Holsteijn
Director a.i. ISRIC-World Soil Information

Summary

This document discusses soil information needs in support of studies of environmental, societal and economic sustainability at an increasingly fine spatial resolution. First, the need for appropriately scaled, consistent and quality assessed soil information in support of studies of food productivity, soil and water management, soil carbon dynamics and greenhouse gas emissions, and the reduction or avoidance of land degradation are discussed. Soil variables considered most critical for current and likely future model-based assessments are identified and new, cost-effective measurement methods that may reduce the need for conventional laboratory methods are evaluated. Following on from this, the status and prospects for improving the accuracy of soil property maps and tabular information at increasingly detailed scales (finer resolution) for the world is addressed. Finally, the scope for collecting large amounts of 'site specific' and 'project specific' soil (survey) information, possibly through crowd-sourcing, and consistently storing, screening and analysing such data are discussed within the context of ISRIC's emerging *Global Soil Information Facilities* (GSIF), together with the institutional implications. GSIF-related activities are currently being embedded in global initiatives such as the FAO-led *Global Soil Partnership*, *GlobalSoilMap.net*, the ICSU World Data System, and the Global Earth Observation System of Systems (GEOSS) that promote participatory approaches to data sharing.

1 Project description

1.1 Rationale

The PBL (Netherlands Environmental Assessment Agency, Bilthoven) project "Ecosystem services and biodiversity" (project nr S550028) assesses, among others, trends in ecosystem services, how these are affected by human interference and how policy interventions could influence trends. Particularly important are the socio-economic consequences of changes in ecosystem service delivery (Figure 1). The awareness of the urgency to assess these consequences has increased as a result of a number of high-key initiatives and studies such as the Millennium Ecosystem Assessment (MEA, 2005) and the TEEB (The Economics of Ecosystems and Biodiversity) project (TEEB, 2008).

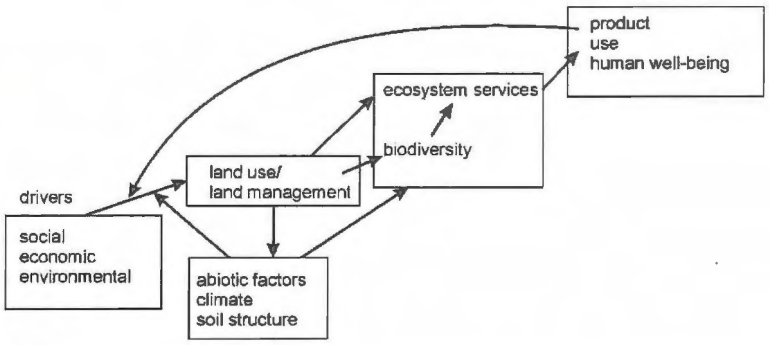

Figure 1

Relations between global change, land use / management change and ecosystem services.

Soils have a key role in the delivery of several ecosystem services, including carbon storage, water regulation, soil fertility and food production (Figure 2). To account for this role in assessments of future changes in ecosystem services, impacts of land use change and other biotic, abiotic and socio-economic factors on soil structure, nutrient availability, hydrology and soil organic matter dynamics should be included in the models used for such assessments. Also, the feedbacks of changes in soil characteristics into crop production and other ecosystem services should be included. This would not only concern on-site effects, but also effects on the wider environment, such as river basin hydrology or conversion of natural areas into agriculture as a consequence of degradation of agricultural areas elsewhere. So far, however, these aspects are hardly considered in global change models. This also applies to the current PBL modelling suite, i.e. IMAGE (Integrated modelling of global environmental change) (Bouwman *et al.*, 2006; Alkemade *et al.*, 2009) and the LPJ (Lund-Potsdam-Jena) vegetation/crop modelling suite (Sitch *et al.*, 2003; Bondeau *et al.*, 2007) that has been linked with IMAGE[1].

[1] Some aspects related to feedback between greenhouse gas emissions, climate change and carbon storage are accounted for in IMAGE.

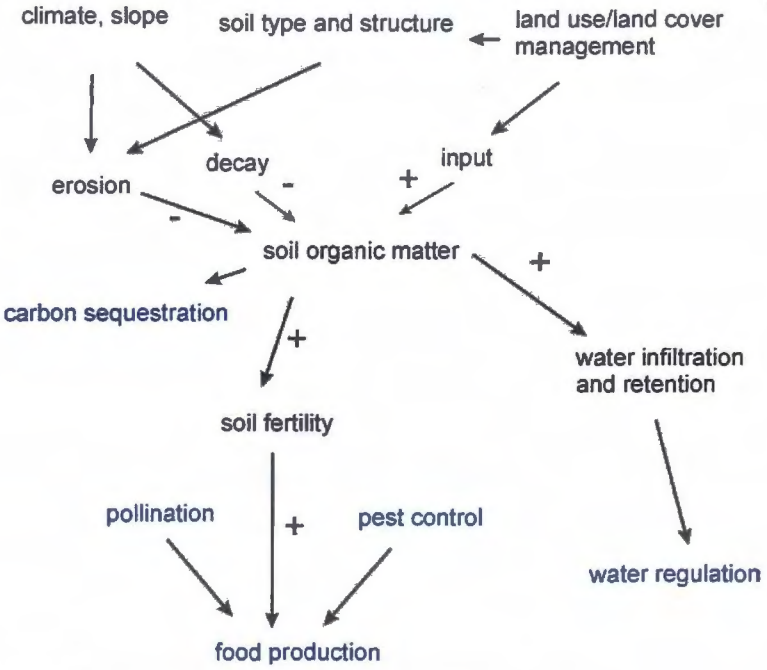

Figure 2

Relations between land use, soil processes and ecosystem services.

About a decade ago, a first attempt was made to model water-induced soil erosion in IMAGE, in a joint project with ISRIC (Batjes, 1996; Hootsman *et al.*, 2001). A simple methodology was used for assessing the risk of water erosion at the global level. That semi-quantitative methodology might be improved by:

- Using improved quality and higher resolution soil data;
- Dynamic modelling of soil changes;
- Quantitative modelling of the impact of soil changes on ecosystem services, including crop production, water regulation and carbon sequestration.
- Improved modelling of processes and impacts of soil degradation will be of great value for the Ecosystem Services project as well as for other PBL initiatives.

1.2 Goals

In this project we assessed the possibilities for improving erosion modelling in the IMAGE framework. We focused on water-induced soil erosion and its impacts on crop production. After that, it would be possible to address other important forms of soil degradation may also be considered. The latter could include, for example, compaction, salinization, nutrient depletion and wind erosion.

1.3 Study set-up

A literature review was made to identify and evaluate all erosion risk assessment models that have been previously used at national scale or broader. Models that seemed to yield a significant improvement relative to the erosion model currently used in the IMAGE framework were evaluated more carefully and in a more quantitative manner. Also, the possibilities for simulating feedbacks with crop production and coupling degradation with the supply of ecosystem services were evaluated. Finally, practical recommendations were given for the improvement of degradation risk modelling within the PBL integrated assessment methodologies.

2 Model review

2.1 Introduction

In this chapter, we present an inventory of erosion models that have been applied at the national scale or broader. Based on a literature review, we describe the structure, outputs and applications of the models and evaluate their adequacy for use within the IMAGE framework.

The IMAGE framework is an ecological-environmental framework that simulates the consequences of human activities worldwide (Bouwman, 2006). It consists of a set of interlinked models to simulate factors such as global circulation patterns, economic changes, land allocation and crop growth. Currently, the LPJ dynamic global vegetation model is being incorporated in the IMAGE framework to replace the existing vegetation and crop growth models. Both the basic LPJ model for natural vegetation and the LPJmL (Lund-Potsdam-Jena managed Land Dynamic Global Vegetation and Water Balance Model) model for managed land are used.

A model for simulation of soil erosion at the global level, suitable for use in the IMAGE framework, should meet the following requirements:

- Provide quantitative outputs that can be used for simulating changes in carbon stock and the soil water holding capacity.
- Be applicable at the global scale. This restricts the spatial resolution to about 5 arc minutes (approx. 10 km) with the current model settings and data availability.

Four groups of models were assessed: models based on the Universal Soil Loss Equation (USLE), the Pan European Soil Erosion Risk Assessment (PESERA) model, regression-based approaches and factor scoring methods. In paragraph 2.2, these groups of models are described and evaluated. Other soil erosion risk models, including LAPSUS (LandscApe ProcesS modelling at mUlti-dimensions and Scales; Schoorl *et al.*, 2002), WEPP (Water Erosion Prediction Project, Gilley *et al.*, 1988)and LISEM (Limburg Soil Erosion Model, De Roo *et al.*, 1996) do not provide possibilities for use at scales larger than a catchment because they are event-based models and simulate sediment flow and re-sedimentation through the landscape. These models require a high resolution, especially for the digital elevation model, which is not feasible at larger scales.

2.2 Evaluation regional and global erosion models

2.2.1 USLE-based models

2.2.1.1 2.2.1.1. Description

USLE

The Universal Soil Loss Equation (USLE, Wischmeier and Schmidt, 1978) is an empirical model, developed by calibrating a conceptual model for soil loss on plot-scale experimental data from the United States. The USLE calculates soil loss by water (sheet) erosion as:

$A = R*K*LS*P*C$ *(equation 1)*

Where

- A = predicted soil loss (ton ha-1 yr-1);
- R = Rainfall erosivity factor. This is a measurement of the erosive force of rainfall in MJ mm ha−1 h−1 yr−1 and expresses the mean annual sum of individual storm erosion rates;
- K = soil erodibility factor, which is a function of soil texture and organic carbon content (t h MJ-1 mm-1);
- LS = factor for slope angle and length (dimensionless);
- P = factor for management practices, including cultivation and soil conservation methods (dimensionless), and
- C = factor for vegetation density and structure (dimensionless).

USLE was designed to predict long-term average soil losses caused by sheet water erosion. It was based on statistical relationships specifically established for croplands in the Eastern US that may not apply elsewhere. It works theoretically best for medium-textured soils, slopes of 3-18 %, slope lengths <400 feet (122 m) and management consistent with measurement plots.

SLEMSA

The Soil Loss Estimation Model for Southern Africa, SLEMSA (Stocking *et al.*, 1988), is based on a combination of factorial scoring methods (Section 2.2.2) and empirical relations with drivers of erosion. It was developed primarily for use at the field scale in Zimbabwe, but with possibilities for application at large scale in mind, with focus on tropical areas. The model formulation is comparable to that of USLE, although the way of combining the inputs is different. While in the USLE all inputs are given the same weight, in SLEMSA more weight is given to the crop factor. When estimating erosion risk with SLEMSA, first an initial erosion hazard index (Ib) is calculated, that combines the rainfall energy (E) and the soil erodibility class (F). Ib is defined as the erosion hazard for bare soil at a 4.5 % slope of 30m long and increases exponentially with increasing rainfall energy and increasing soil erodibility. The final erosion hazard index is calculated by multiplying Ib with a cover factor (C) and a slope factor (X):

$$\textit{Erosion Hazard Index} = I_b * C * X \qquad \textit{(Equation 2)}$$

Inputs for the model at large scale are:

- Seasonal rainfall energy, which is derived from mean annual rainfall through an empirical regression equations for accumulated and individual rainstorm (Kowal and Kassam, 1976; Stocking *et al.*, 1988; Lal, 1982; Marx, 1988).
- Soil type (F-factor). Each soil type-texture combination is classified into a soil erodibility class, ranging from 1 to 10. The erodiblility of most (of Zimbabwe's) soils vary with land use and management (Elwell, pers comm.). The F-factor can therefore be modified on the basis of several factors, such as soil management, internal drainage, lithic contact, abrupt soil textural change, and/or the sensitivity to capping. SLEMSA is very sensitive to these modifiers. More details on this and the modifiers are found in (van den Berg and Tempel 1995).
- Vegetation: A crop-specific cover percentage is used to estimate the proportion of rainfall that is intercepted by vegetation. It is calculated as a non-linear function of rainfall interception and is related to a cover factor that expresses the soil loss ratio relative to bare ground (C).
- Average slope in % and slope length. This is recalculated into a slope factor (X).

The Erosion Hazard Index (EHI) is expressed in Erosion Hazard Units on a scale of 0-1000. According to Stocking *et al.* (1988) these should not be interpreted as soil loss in tons per ha.

The main differences between SLEMSA and USLE are that in SLEMSA, the management factor (P) of USLE is left out, because it was felt that the effect of local conservation practices can be allowed for in the slope factors (L or S) within the topography system, or in the erodibility (F) in the soil system. The other factors are quantified by methods which are simpler to calculate or require less data. The rain erosivity factor (R) in USLE is replaced by a measure of the total annual kinetic energy of the rainfall, which is easier to calculate from rainfall records (Stocking *et al.*, 1988). In the USLE, the cover factor (C) is expressed as a ratio of the soil lost from a vegetated plot to the soil loss of an identical plot under clean-tilled, continuous fallow. Average annual values are available for different crop and management systems. In SLEMSA, the cover factor is instead defined as the percentage or rainfall intercepted. This is exponentially related to the cover percentage (i). The soil erodibility factor based on texture and organic carbon content (K in USLE) is replaced by a soil erodibility index (F) in SLEMSA based on soil type and texture. The relief factors (LS in USLE and X in SLEMSA) are calculated in a very similar manner.

2.2.1.2 Applications

The USLE is the most widely used model for predicting water erosion hazard because it is an easy to use and transparent model with low data requirements (Sonneveld and Nearing, 2003). On a large scale, USLE has been used for assessing spatial patterns of soil erosion in Australia (Lu *et al.*, 2001), Europe (Eickhout *et al.*, 2008) and on global scale (Hootsmans *et al.*, 2001; Pham *et al.*, 2001). Dependent on the scale of analysis and the data availability, it has been simplified or extended. In hill slope or plot-scale studies, parameters are derived from measurement-based calibration. At larger scale, the parameters are derived from aggregated data. Slope characteristics, for example, are derived from large-scale digital elevation models (DEM's) and the K factor is estimated using a continental soil map and pedotransfer functions (Hootsmans *et al.*, 2001). The study for Australia accounts for the large intra-annual variability of precipitation by calculating erosion per month using monthly rainfall and monthly vegetation cover data (Lu *et al.*, 2001). At national and regional scale, the USLE or USLE-based methods have been used for risk assessments in Germany, Spain, Finland, Hungary, Belgium, Norway, Europe (Geraedts *et al.*, 2008) and in Kenya, Zimbabwe, Uruguay and Argentina (Mantel and Van Engelen, 1999 and Mantel *et al.*, 2000), and Indonesia (Tyrie and Gunawan, 1999).

In IMAGE (Bouwman *et al.*, 2006, Hootsmans *et al.*, 2001) a USLE based 0.5o x 0.5o assessment of erosion sensitivity is included. The USLE is simplified by aggregating the soil erodibility and slope factor into one terrain factor (Section 3.3.1). Erosion risk is translated into categorical output (no/low – moderate – high – very high).

The SLEMSA model was developed for Zimbabwe (Stocking and Elwell 1973a; Stocking and Elwell 1973b; Stocking, Chakela *et al.* 1988; Elwell 1990; Grohs and Elwell 1993) and was applied to assess erosion in Lesotho (Chakela *et al.*, 1988). SLEMSA has been applied in (Southeast) Africa only. In the Lesotho case (Chakela et al, 1988), the erosion hazard is reclassified into classes 4 (high; EHU = 51-100) to 8 (extremely high; EHU >1000) using an exponential scale.

2.2.1.3 Quality issues

Sonneveld and Nearing (2003) investigated the robustness of the USLE using cross-validation techniques. Cross-validation of USLE simulations against the original calibration dataset resulted in an R2 of 0.57. Model parameters were not very robust; the cross-validation indicated deviations of up to 15% for the slope (LS) factor and up to 100% for the management (P) factor. When all six input parameters are combined by multiplication with equal weights, large errors may be propagated in the final outputs.

Albaladejo Montoro (1989) compared plot-scale USLE and SLEMSA erosion assessments with measured erosion rates. In his study, USLE estimated erosion rates were of the right order of magnitude, but with a too low spread of values, while SLEMSA was better in predicting spatial patterns of differences, while underestimating the quantity of erosion. Also Stocking *et al.* (1988) point at the underestimation of erosion. This is probably due to the aggregation of slope and rainfall data by using mean values. The approach of SLEMSA seems to be applicable for a somewhat wider range of soils than the USLE, and also works for slopes up to 20%.

The global-scale spatial patterns of erosion risk as simulated with the USLE-derived model used in IMAGE have been compared with GLASOD, a global, expert-judgement based, assessment on the human-induced status of soil erosion and degradation. Visually, the agreement seems to be quite well (Hootsmans *et al.*, 2001). GLASOD represents the actual status of soil degradation (in '80-'90), while the global USLE assessment indicates the risk of soil erosion under actual conditions and therefore results are not necessarily compared.

Conceptual flaws in the USLE, as indicated by Kirkby *et al.* (2004), include mainly the proper distinction of soil and climatic conditions in the infiltration process. Most of these limitations would also apply to SLEMSA, because the soil and rainfall factors are combined in a similar way.

2.2.2 Factor scoring methods

2.2.2.1 Description

Factor scoring methods are empirical models that estimate an erosion risk index based on expert knowledge. In a factor scoring method, parameters that influence the erosion risk are scaled into a semi-quantitative index for their importance for erosion risk. By combining indices for all parameters relevant in the area under study, a general indication of the erosion risk is obtained. Generally, factor scoring methods result in qualitative or semi-quantitative indications of erosion risk. Four main inputs are generally considered in modelling of erosion: soil, topography, land cover and rainfall. Indices can be combined by calculating a (weighted) average, multiplying separate factors or using a decision tree.

2.2.2.2 Applications

Factorial scoring methods are commonly used for country-scale assessments of erosion risk (Geraedts *et al.*, 2008). The French Agronomical Research Institute (INRA) developed a factorial scoring method for erosion risk (Le Bisonnais *et al.*, 2002) that has been applied in France and in the EURURALIS project (Klijn *et al.*, 2005). With this method, a soil map is classified into three classes of erodibility and four classes of crusting risk. A DEM of Europe is classified into eight slope classes based on average elevation differences with the eight neighbouring cells. Current and future land use is simulated with the CLUE model, distinguishing nine classes of land use (Verburg *et al.*, 2006). Each class is given an erosion sensitivity rating. Annual average rainfall and frequency of exceeding 15 mm d-1 are simulated using the IMAGE framework and classified into five erosivity classes. Indices for erodibility, crusting, slopes, land cover and rain erosivity are then combined into a single index using a decision tree. The index was used to visualize potential changes of erosion risk upon changes of climate and land use (Klijn *et al.*, 2005).

De Vente *et al.* (2008) compared sediment yields observed in 61 catchments throughout Spain with those simulated with different models, including the Spatial Distributed Scoring (SPADS) model. This is a factorial scoring model that simulates sheet, rill, gully, channel and landslide erosion. Factor scorings for different factors influencing erosion are translated into a range of soil loss.

2.2.2.3 Quality issues

A common criticism to factor scoring methods is that model formulation is subjective. Parameters may be given more weight, depending on the goal of the study and therefore predictions may be inconsistent. Prediction of uncertainty can be done when the uncertainty in the input parameters is known. Generally, factor scoring methods provide qualitative outputs although for specific case studies a factor scoring model can be calibrated so that soil loss can be estimated (De Vente *et al.*, 2008). In spite of the criticisms named above, in the study by De Vente *et al.*, the SPADS model explained 67% of variation in sediment yield in the studied catchments and outperformed the other models under study.

2.2.3 Regression-based methods

2.2.3.1 Rationale

Regression-based models are empirical models to estimate erosion rates based on a statistical relation between sediment yield or soil loss and site characteristics. A regression equation is fitted to the data on sediment loss and site characteristics and the equation is then used for upscaling. Common independent variables included in such regression models are land use, topography and lithology, and climatic conditions.

2.2.3.2 Applications

In the NEWS-PNU model (Beusen *et al.*, 2005) sediment yield at the outflow of watersheds is modelled as a function of watershed characteristics. Sediment yields from a global-scale dataset were used for calibration and validation. The model aims at predicting fluxes of suspended sediment, organic carbon, particulate N and particulate P to coastal waters. Independent variables include fractions of the basin covered by certain land use systems, soil texture and slopes. The model estimated sediment yields with an R2 of 0.60. Lithology of the catchment was the main factor influencing sediment yields.
A regression approach allows analysis of the factors that influence sediment yield in a catchment. Such information could be used directly for upscaling in space and time or serve as a basis for the development of an empirical model. With the use of input data for scenarios of environmental change, the impact on sediment yield may be estimated (Syvitski *et al.*, 2003). Upon application of the NEWS-PNU model in future scenario simulations one should note that the impact of factors may change when the model is applied for conditions other than those for which the model was developed.

2.2.3.3 Quality issues

The robustness of NEWS-PNU was tested with cross-validation. The NEWS-PNU model prediction for the total suspended sediment flux for 3107 rivers across the globe, as calculated by Beusen *et al.* (2005), is:
12.9 Pg y-1. The 97.5% upper boundary is 18.9 Pg y-1, which is a factor of 1.5 of the prediction (Beusen *et al.*, 2005). Probably, presence of interaction between the factors is included in the regression model, which is often not explicitly accounted for. The output of NEWS-PNU represents total suspended sediment fluxes out of a basin. The results cannot be downscaled within the basin, so the results are not really spatially explicit.

2.2.4 PESERA

2.2.4.1 Rationale

PESERA (Pan–European Soil Erosion Risk Assessment) is a physically based spatially explicit erosion model. It was developed for quantifying soil erosion in environmentally sensitive areas relevant to a European scale and for defining soil conservation strategies (Kirkby et al, 2004).

Two version of the PESERA model exist: a point model and a regional model. PESERA was first developed to simulate the sediment transport for a single storm at the scale of a single hill slope. Thereafter, PESERA has been scaled up to simulate long-term average soil loss at the European scale. For this, daily rainfall rates are integrated over the frequency distribution of daily rainfall events. Then, sediment loss is calculated using a power law, corrected for vegetation cover and soil erodibility. Output of PESERA is the long-term average soil loss from runoff discharge and gradient, at the base of a hillside.

PESERA uses mean monthly climate data for reasons of data availability and to simulate long-term average conditions. With a gamma function, the monthly frequency distribution of rainfall is simulated. The coarse temporal resolution of climate data, excludes the use of infiltration calculations based on Richards' equation and a runoff threshold approach (bucket model) was chosen instead (Kirkby, *et al.*, 2008).

In the PESERA model concept first stable hydrological and vegetation conditions are assessed under given climate. These conditions are subsequently used to calculate mean monthly erosion rates. To this end, equations are solved iteratively to calculate hydrological and vegetation-related parameters in an annual cycle until stable conditions are reached. These equations are solved independently for each raster cell. Neighbourhood relationships are not considered (Kirkby *et al.*, 2008).
The PESERA model runs on climate, soil, land use, and relief data. The standard input and output variables for the PESERA model are summarized in Tables 1 and 2, respectively.

Table 1

PESERA Input Parameters .	**Input Parameter**	**Source Data base (1km)**	**Explanation**
Climate	Mean Monthly Rainfall (mm) Mean monthly Rain/rainday (mm) Coefficient of Variation of rain/rainday Mean monthly temperature Mean monthly Temperature range Mean monthly Potential evapotranspiration (PET)	BADC[a]/ MARS[b]	Preferably, data extracted from extended record of daily rainfall, PET and climate data from weather stations within and around the target areas are used
Soil	Soil water storage capacity (this is the maximum capacity of soil before runoff) Profile depth of soil textures (Zm) Crusting Erodibility	SGDBE[c]	Currently, soil parameters are derived from texture and physical-chemical data from pedotransfer rules
Land Use	Planting month, harvest month Water Use Efficiency Land cover Root depth Initial surface storage Surface roughness reduction per month	SGDBE[c], Corine	Land-use-classification
Relief	Standard deviation of elevation in 1.5km radius	Gtopo30 DEM	30m global DEM

Source: (Kirkby, Irvine *et al.* 2003; Kirkby, Irvine *et al.* 2007)
[a] British Atmospheric Data Centre, UK Natural Environment Research Council (http://badc.nerc.ac.uk/)
[b] Monitoring of Agriculture with Remote Sensing, EU Joint Research Centre (http://mars.jrc.it/)
[c] Soil Geographical Data Base of Europe (Ref)

Climate data preferably consist of a record of up to 50 years of daily values for individual stations. A high density of actual rainfall station data is particularly important. For producing the PESERA map, the MARS agro-meteorological data were used, interpolated to 50 km resolution.

The soil parameters for PESERA may be derived from soil mapping units, interpreted as textural data and converted to parameter values using pedo-transfer rules. Soil parameters required include soil moisture variables (soil water storage (Surface storage is equal to soil roughness storage in mm water that remains on surface of soil plus soil storage in mm, which is the internal water storage capacity) and scale depth (the depth of soil textures in the profile), soil surface properties (crust storage), and erodibility. Surface storage is equal to soil roughness storage (mm); water that remains on surface of soil plus soil storage (mm), which is the internal water holding capacity. Scale depth is an indicator of the depth in the profile of the soil texture class. For creation of the Pan-Europe erosion risk map the soil geographic database of Europe (SGDBE) was used that provides a harmonised and spatial coverage of soil types and descriptions at a resolution of 1:500,000 (c. 1km x 1km) (European Soil Database: JRC, 2001).

As input for land use, the land cover percentage and the type of crop are used. From this, a rooting depth and a surface roughness is specified.
As relief input, PESERA uses the standard deviation of elevation in a radius of 1.5 km around each grid cell. A Digital Elevation Model, Gtopo30, provides the required relief data for PESERA at approximately 1 km resolution with global coverage.

Output of the PESERA model includes hydrological, erosion and vegetation parameters, summarized in Table 2.2. This provides a wider range of properties to be used in analyses of ecosystem services then just the output of risk of soil loss.

Table 2
Typical monthly output variables for each cell in the PESERA model.

Output parameter **Description**	**Units**
Erosion (monthly)	ton ha^{-1}
Overland flow runoff (monthly)	mm
Soil water deficit (monthly)	mm
Percentage interception (monthly)	%
Vegetation biomass (monthly)	Kg m^2
Cover (monthly, if not pre-set by land use)	%
Soil organic matter (monthly)	Kg m^2

Source: (Kirkby *et al.* 2003; Kirkby *et al.* 2007).

2.2.4.2 Applications

The PESERA regional model has been used to calculate long-term average erosion rates over Europe (Kirkby *et al.*, 2004). It was developed for use at the 1 km resolution. Where local data are available at higher resolution, these can be utilized at the user's discretion. However, as data resolution is refined (< 100 m grid resolution), assumptions applied in the development of the PESERA model may not hold (Kirkby, Irvine *et al.* 2007). Although PESERA was developed for Pan-European conditions, it has also been tested and applied in North African conditions and 16 sites in dry land test areas test areas around the globe (Fleskens *et al.*, subm.).

2.2.4.3 Model evaluation

Although the lack of direct soil erosion measurements for large areas (supra-national) hampers a thorough validation or cross-validation, PESERA was applied and tested at various scales for areas in the European Union. Van Rompaey *et al.* (2003) assessed the accuracy of PESERA, USLE and a factor scoring model developed by the INRA. Soil erosion data derived from sedimentation volumes in reservoirs in Belgium, the Czech Republic, Italy and Spain were compared with the model outputs. This study showed that the PESERA model did not produce accurate erosion predictions for all European environments at 1km resolution. The relative pattern of soil loss from agricultural areas in central Belgium and the Czech Republic was modelled adequately. The model could however not accurately predict the observed soil erosion patterns in Italy and Spain (Van Rompaey *et al.*, 2003). The main reasons mentioned were:

1. Uncertainty involved in the indirect validation method (i.e. sedimentation data in reservoirs);
2. Low resolution of the input data used for model applications at European scale;
3. Simplified internal model structures that do not take into account all sediment producing and transporting processes.

Van Rompaey *et al.* (2003) state that past research has shown that some models perform much better for areas when higher resolution input data are used. Runoff was based on a 1x1 km grid in their study. De Vente *et al.*, (2008) compared the performance of PESERA, SPADS (section 2.2.2) and the USLE-based WATEM-SEDEM model in 61 catchments across Spain. In this study, PESERA soil erosion rates are of the same order of magnitude as erosion rates measured in erosion plot studies. Yet, for many basins sediment yield could not be explained by PESERA erosion output. This is probably mainly because PESERA does not include erosion through stable long-term gullies. De Vente *et al.* (2008) also expect that model performance of PESERA can improve by using better soil data and a DEM with higher resolution.

Geraedts *et al.* (2008) compared 11 methods that have been used for assessment of soil erosion risk in Europe. They evaluated if the scale of processes included in the model are commensurate with the available data, model transparency, complexity, cost efficiency and reliability of the results. PESERA is considered transparent because of the physics-based approach, i.e. process based equations that are based on the relation between runoff and sediment detachment. Scale and complexity are rated intermediate, while cost efficiency and ambiguousness of the results are rated low in this study.

Licciardello *et al.* (2009) evaluated the performance of PESERA using field data from 30 plots in Italy and The Netherlands and assessed the effect of all model components on prediction accuracy. They evaluate the prediction of annual average erosion rates by PESERA as adequate, especially at rates > 1 ton ha-1 yr-1. Short-term temporal variations are not captured well. Major causes are the unrealistic simulation of runoff and cover but also the erosion prediction itself causes errors. Variability between land covers and climates is well captured, but the model generally strongly underestimates actual erosion rates. The authors propose further calibration of the model. The underestimation is also found by Meusburger *et al.* (2010).

Meusburger *et al.* (2010) compared PESERA and USLE erosion estimates with in situ measurements of erosion rates in alpine grasslands. In this study a 25 m DEM was used (DEM ©swisstopo). The study uses fractional vegetation cover (FVC) which is the fraction of the surface covered by vegetation. While the USLE uses an empirical factor for the effect vegetation cover ($C = 0.45 \times e^{-0.0456 \times cv}$), PESERA uses a vegetation growing module to estimate cover fraction. Both models were applied at 0% and 100% FVC and at the observed FVC.

Both models underestimated the erosion rates. PESERA estimations were far too low, even lower than the USLE predictions, despite the fact that PESERA takes snow accumulation and snow melt into account (peak erosion occurs during snow melt). Compared to USLE, PESERA underestimated the importance and influence of vegetation cover on soil erosion in alpine grasslands. Both the spatial pattern of erosion was poorly reproduced and the absolute amount of erosion was underestimated compared to the in situ measurements and lower than predicted with the USLE. Input of high resolution vegetation cover data significantly improved erosion rate estimations.

Possible reasons for underestimation of erosion rates by PESERA under low FVC are (Meusburger, *et al.* 2010):

4. Lower sensitivity of PESERA to differences in FVC, which results in a very narrow range of erosion estimates;
5. Low erosivity resulting from monthly averaged climate input data in PESERA that smoothes out extreme events. Even though a coefficient of variation for the monthly precipitation is considered, its impact on soil erosion estimates is small. The empirical basis of USLE, where the impact of FVC is implemented via the C factor seems more suitable than the vegetation growing module of PESERA on the site researched (Meusburger, Konz *et al.*, 2010).

In a study done for Zakynthos in Greece (Tsara *et al.*, 2006), the measurement from erosion plots under various forms of cover and management were compared with PESERA outputs. Existing erosion data from the same area were used for comparison. Data were collected at two locations, but along various transects and plots on each of the locations, amongst other for various land uses. Model performance was best for the erosion plots on bare, stony land. Comparison between the outputs obtained from the PESERA model and the measured values in the various soil erosion plots generally showed a satisfactory performance by the model. Rates of soil erosion were better predicted for the abandoned bare land with a maximum error of 0.65 t ha-1 yr-1. Overall predictions of the PESERA model seemed to be in reasonable agreement with the measured values of soil erosion for the test sites in Greece. The overall efficiency of the model (Nash and Sutcliffe, 1970), was assessed using the available erosion data. The model efficiency2 was relatively good (0.69), even though the maximum error3 of 1.49 t ha-1 yr-1 may be considered high, depending on the purpose of modelling and the land vulnerability.

Kirkby *et al.* (2004) indicated in that the coarse spatial resolution of climate data was the most critical shortcoming of the Pan-European Erosion risk assessment.

2.3 Conclusions

In Table 3, strengths and weaknesses for all four types of models are summarized. With a focus on global-scale applications. For such applications, low data requirements are an asset and the model should be able to handle the global range of vegetation types, slopes, climate- and soil conditions.

---

2 A statistical measure of model forecasting efficiency introduced by Nash and Sutcliffe (1970) and proposed by Loague and Freeze (1985) that is based on predicted values, observed values, and overall mean values. Based on a sum of squares criterion, the maximum value for model efficiency is one. A value that would be reached only if the observed and computed runoff variables were identical. A negative efficiency indicates that the models predicted values is worse than simply using the observed mean (Loague, 1982)

3 The maximum error represents the single largest difference between a pair of predicted and observed values.

Table 3

Strengths and weaknesses of erosion models.

	Strengths	Weaknesses
USLE /	– Data requirements are low	– Based on regressions of local conditions – Representation of infiltration process
SLEMSA	– Versatile: Can be easily adapted to the data available, or to a specific case study – Can provide quantitative outputs – USLE is a well-established often used model, also at global scale	– Not robust: when used outside the standard boundary conditions the outputs may strongly deviate – Quantitative outputs cannot always be interpreted as such, especially at larger scales
FACTOR SCORING	– Data requirements are low – Simple and versatile. E.g.; easy to adapt to the available data and a specific model can be easily made to assess specific kinds of erosion	– Qualitative outputs only or extensive calibration needed – Choice of model parameters is subjective and therefore inconsistent – No global-scale applications available
REGRESSION BASED MODELS	– Helps in providing insight in factors controlling the sediment load in a basin – Versatile data requirements	– Low resolution: Generally only catchment-specific at large scale – Difficult to make universally applicable – Sensitive to over-parameterization
PESERA	– Transparent – Good representation of effect of climate and land cover: good for simulating future changes	– Generally underestimates erosion in case studies throughout Europe, *indicating incomplete representation of erosion processes* – High data requirements, time-consuming calculations. – Sensitive to DEM and climate data resolution. – No global-scale applications available

The IMAGE framework comprises a USLE-based index for assessing erosion risk (Section 2.2.1). Currently, it is not possible to estimate soil loss rates and effects on plant productivity for different water erosion processes at the scale of IMAGE calculations. Another problem is that it is not possible to translate soil loss rates into effects on soil productivity as a result of loss of physical stability or chemical fertility (Hootsmans *et al.*, 2001). Spatially explicit high-resolution simulations of erosion risk are needed for this and the feedback of soil loss on productivity should be explicitly included.

Regression-based models typically provide outputs per catchment and thus have a too coarse resolution to be suitable for our goals. A main problem of factor scoring methods is that they either provide a categorical output that cannot be translated into quantitative estimates of soil loss and changes of productivity, or need data-intensive calibration which is not feasible at global scale. Therefore, this method is not considered an improvement compared to the USLE. SLEMSA has not been used outside of Africa and has not been used by the scientific community after 2000. In a comparison with the USLE, it did not perform better. Therefore, SLEMSA is not considered an improvement relative to the USLE. PESERA has the advantage of a process-based approach that might be globally applicable. Although the model has never been used outside Europe and tends to underestimate erosion risk. Nonetheless, due to the structure and outputs of the model we considered that it might be an improvement relative to the USLE. Therefore, the possibilities for applying PESERA at global scale within the IMAGE framework are assessed in more detail and a comparison with the USLE as currently used in the IMAGE framework was made.

3 Effect of DEM resolution scale on model output

3.1 DEM aggregation

3.1.1 Introduction

Topography defines the effects of gravity on the movement of water and sediments in a catchment. Therefore, digital elevation models play a considerable role in hydrologic simulation, soil-erosion and landscape-evolution modelling (Zhang *et al.*, 1999). Slope is a key factor in hydrological and erosion modelling (Beven and Kirkby, 1979; Freedman *et al.*, 1998) and is commonly derived from DEMs. Consequently, erosion models are known to be sensitive to DEM resolution (Zhang *et al.*, 1999, Claessens *et al.*, 2005); estimates of slope values and slope variability change with DEM resolution. Zhang *et al.* (1999) found that slopes calculated for a specific area from DEMs with varying resolution are inversely related to DEM grid size, meaning that slopes estimated from coarse resolution data can be considered to produce significant underestimates of the true slope. The critical parameter in the PESERA model is local relief, which has been estimated from DEMs as the standard deviation of altitude. Comparisons with DEMs at resolution from 1000 m down to 30 m showed that this measure is insensitive to DEM resolution, and can therefore be used reliably with the best DEMs available for each area (Kirkby *et al.*, 2004). The standard deviation of altitude is estimated from DEMs within a square of 3 km around each 1 km x 1 km cell (3x3 window). The latter is what is called focal statistics: it analyses adata raster using a moving neighbourhood region. It returns a raster, each cell value expressing a summary of the data grid for the neighbourhood centered on that cell (Tomlin, 1990).

3.1.2 Methods

No studies are available of the PESERA model applied to global scale data. Therefore a comparison was made of different methods of DEM aggregation and their impact on model output. The PESERA model was run on DEMs of different resolutions. These DEMs were developed using two different methods. In this way, the effect of DEM scale difference on PESERA output was studied. Furthermore, the impact of the different methods of DEM aggregation on the model output was assessed.
The 90m DEM was aggregated to 1km by calculating the mean altitude per grid cell for a 1 km mesh. Two methods, A and B, were tested to derive the 1 and 10 KM DEM grids.

Method A
From the 90 m SRTM DEM, three DEMs were created: 1 km, 5, 10 km resolution. First, a bilinear resampling[4] was done on the SRTM 90 m. Then the grids where aggregated to a 5 and 10 km resolution. The standard deviation of altitude was calculated for all surrounding cells of one pixel from the 90 m DEM (3X3 cell block; 3x3 km, 15x15 km and 30x30 km. This procedure results in weighted average values, based on distance
(Figure 3).

[4] bilinear resampling is a method for geometric correction. A regular grid of desired dimensions is overlaid and based on the values of the original grid, values are calculated for the new output grid. The new values are derived from a distance weighted average of the values from the four nearest pixels in the original input grid.

Method A:

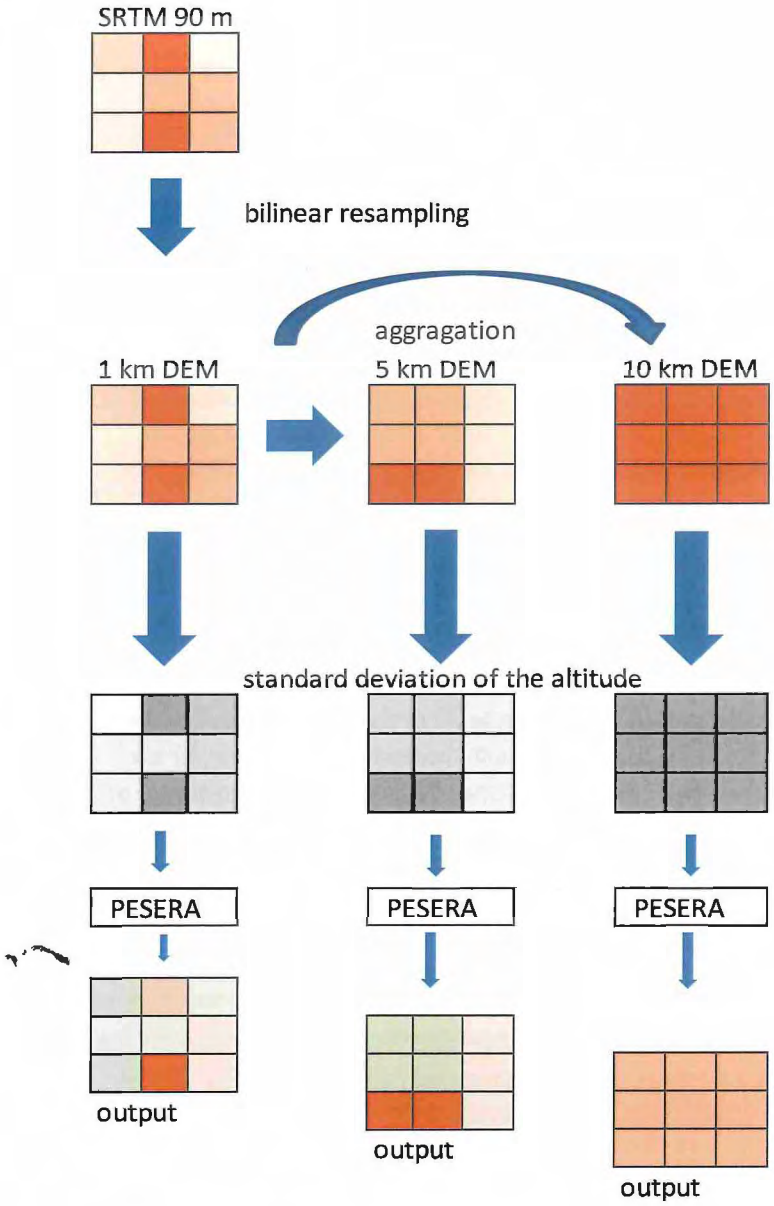

Figure 3

Creation of DEMs at 3 resolutions using method A.

Method B

This method differs from method A, in that the standard deviation for the 10 km grid was calculated by averaging the standard deviation of all 100 pixels of 1 km2 in a 10 km x 10 km grid cell (*Figure* 4).

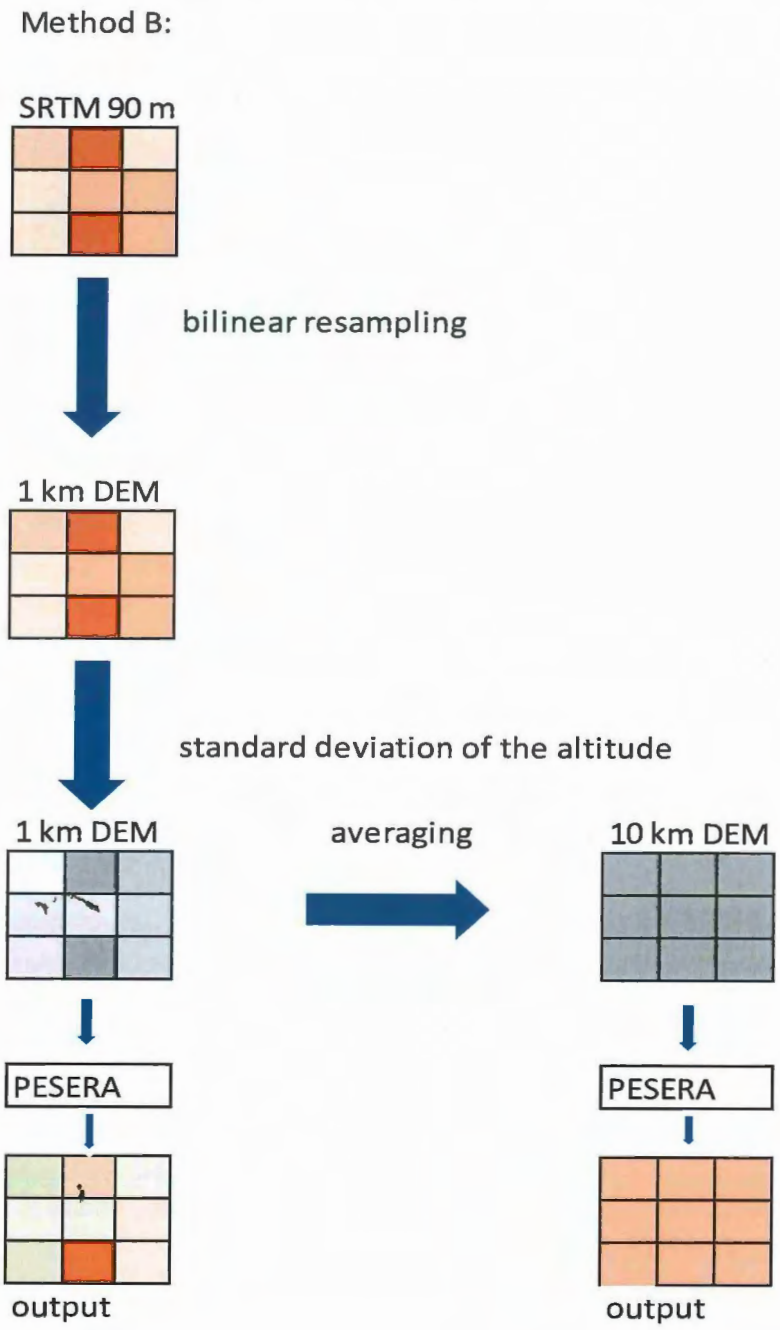

Figure 4

Creation of DEMs at 3 resolutions using method B.

3.1.3 Results: DEM Aggregation on PESERA output

In this section the results using method A is discussed.

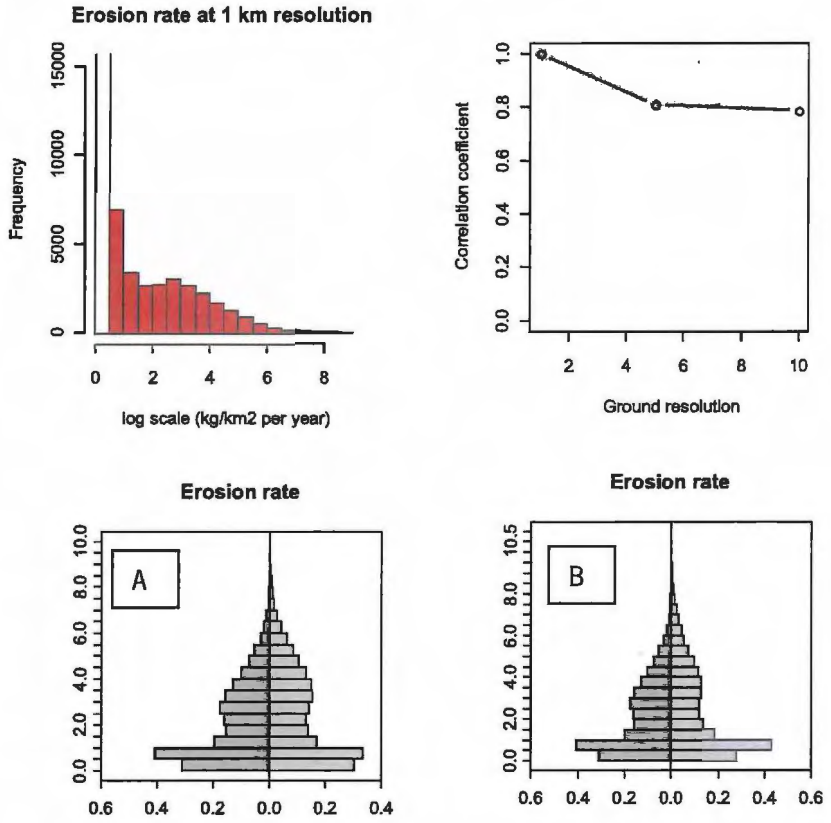

Figure 5

Comparison of PESERA output run of DEMs of 1, 5 and 10 km resolution (method A).

The correlation coefficient between the outputs of PESERA for the three different resolution DEMs (method A) are high (approximately 80%). When comparing histograms of the 5 and 10 km DEM with that of the 1 km (Fig 5 A: 1:5 km and Fig 5B: 1:10 km) it is noted that the ' belly' of the 5 km is higher than that of the 1 km grid indicating that the 5 km DEM has more grid cells with higher PESERA erosion output values. The 1 km has most values in the lower to middle erosion classes, while the run on the 10 km DEM has a more evenly distributed frequency over the classes with the highest in the lower class, but also more high values as compared to the 1 km DEM.

Figure 6 shows a detail of three DEMs in three different resolutions.

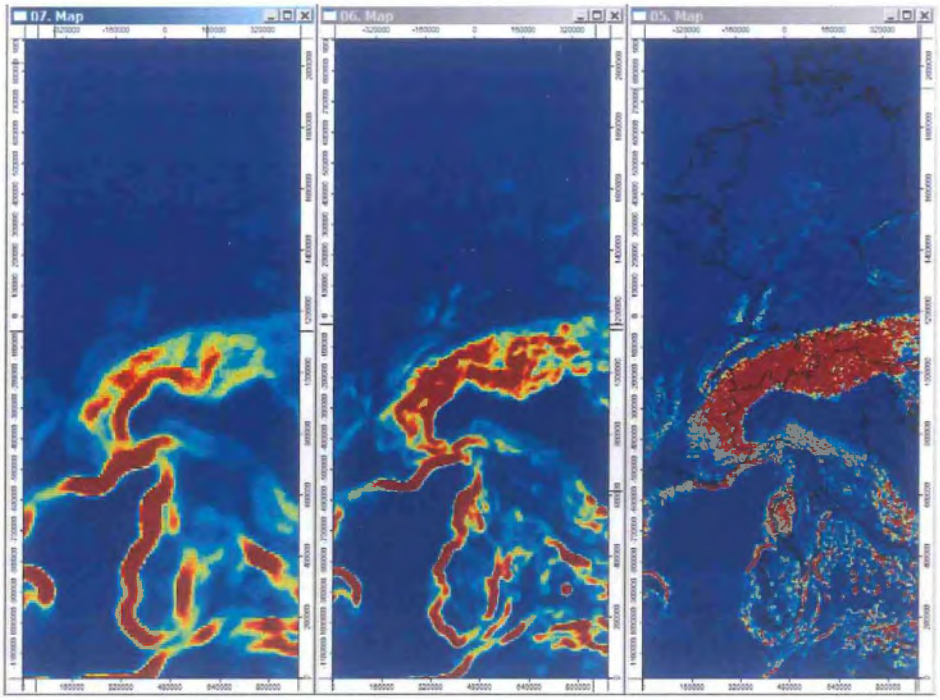

Figure 6

Detail of DEMs of different resolutions (10, 5, and 1 km).

Figure 7 represents the value of sediment output of PESERA run on the 10 km DEM, minus those for the 1 km DEM. The former are clearly higher in the Mediterranean and mountainous areas of Europe. The standard deviation of the altitude is higher in the mountainous areas and in transition zones between land units. In a larger grid the standard deviation of the altitude is then even higher.

Figure 8 shows the kappa statistics of the comparison between the PESERA runs on the three different DEMs. The figure shows that the 1:1 line is visible but with a cloud of deviating values. A second line is visible that shows a range of values where the PESERA outputs on the 5 and 10 km DEM are higher and the run based in the 1 km DEM are in the lowest class. Alternatively, between the 1 km and 5 km grid the reverse trend is also visible (higher 1 km based PESERA outputs for lowest class 5 km grid) but less clear for the 10 km based run. This shows that with the coarser resolution DEMs there is a systematic error towards higher values. As shown in Figure 5 that shows erosion calculated based on the 1 and 10 km DEM in kg.m-2.yr-1.

When comparing the two maps (*Figure* 9) it is clear that the patterns are the same for the two maps, but that the intensity of the predicted erosion is higher for the 10 km map.

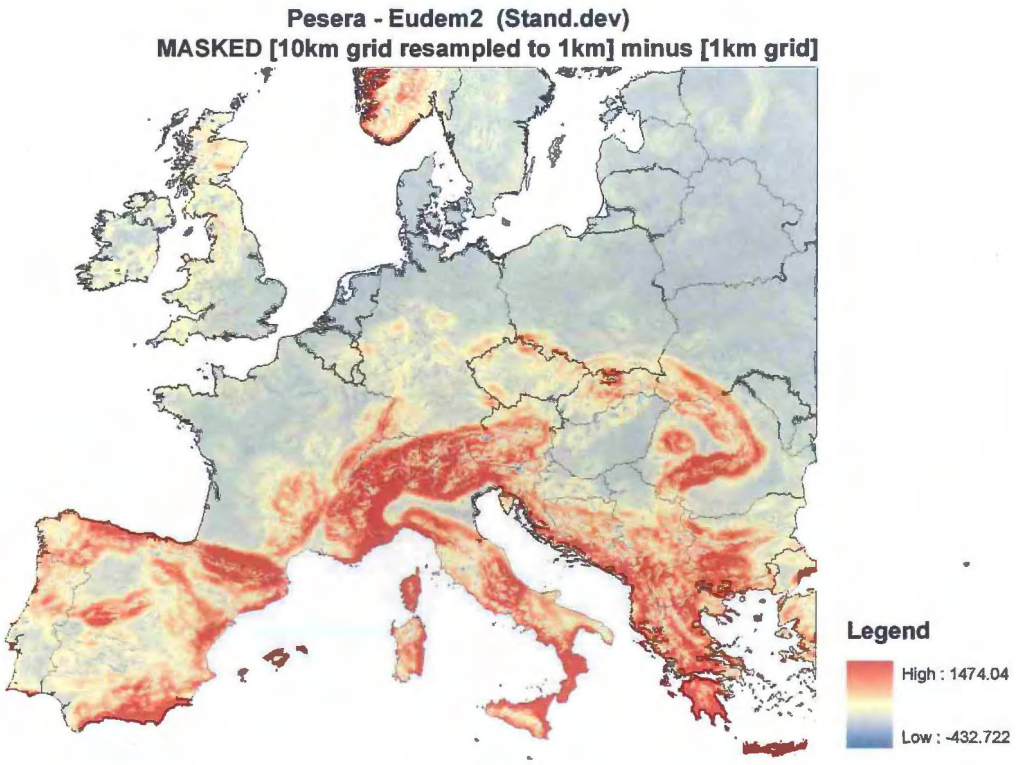

Figure 7

Comparison of PESERA output using a 10 km DEM with that run on a 1 km DEM.

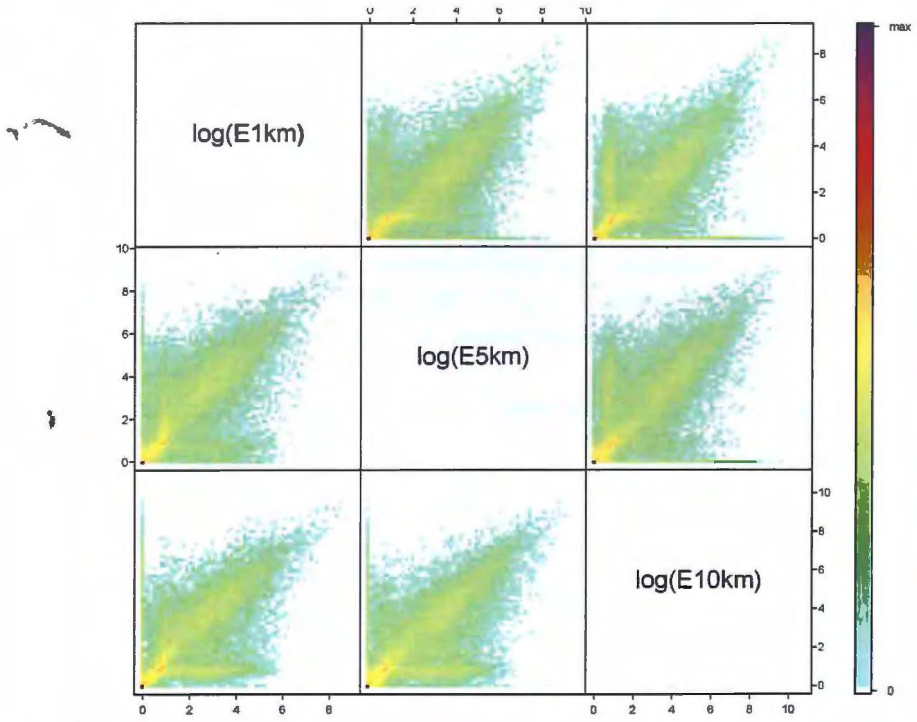

Figure 8

Kappa statistics diagram of PESERA output based on three resolution DEMs.

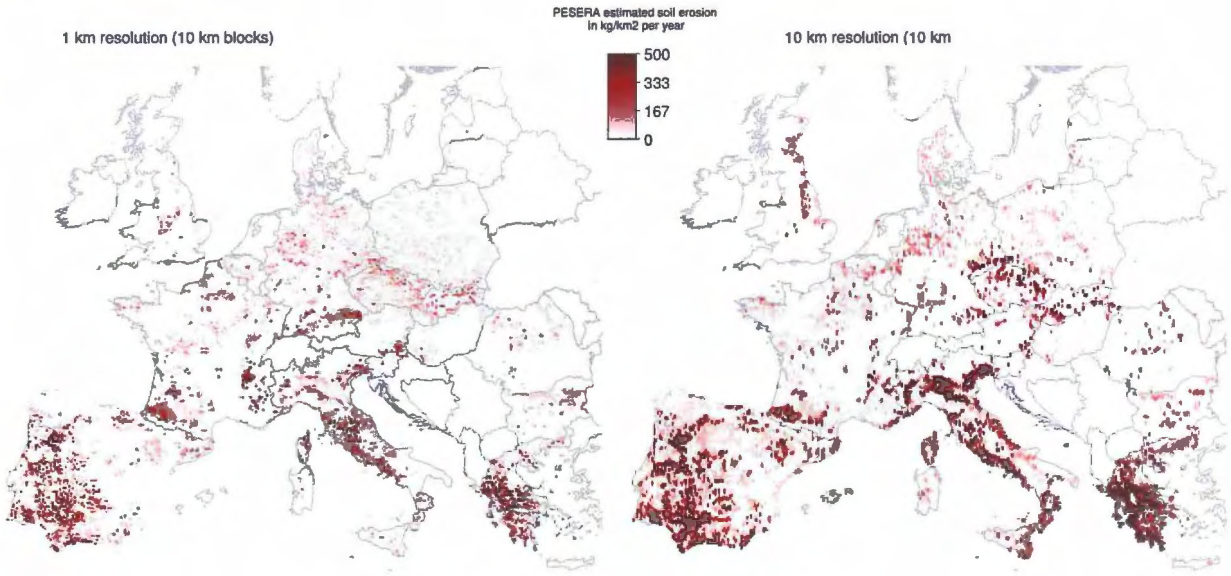

Figure 9

PESERA estimated soil erosion (kg.m^{-2}.yr^{-1}) based on 1 and 10 km DEM.

In conclusion, with method A, the mean altitude is aggregated over 1 km and 10 km grid cells, after which the focal standard deviation is calculated using surrounding 3x3 cell grid blocks. The advantage of this method is that both the 1 km and the 10 km grids are created following the same methodology. A systematic error is however created in the lower resolution DEM, when the standard deviation of the altitude is calculated for larger grid cells. The standard deviation is calculated of larger areas as compared to the higher resolution grid. As the same DEM source is used for both resolution grids the standard deviation will generally be higher when assessed over larger block (grids). This trend is visible in the results of PESERA run on the two grids and most clearly visible in figure 9.

Method B

Using method B, only 1 km and 10 km resolution DEMs were compared. Figure 10 presents the spatial distribution of the standard deviation of altitude. It shows that the pattern is similar with a smoothened surface for the 10 km grid as a consequence of the resolution effect. Magnitude and pattern seem consistent with each other.

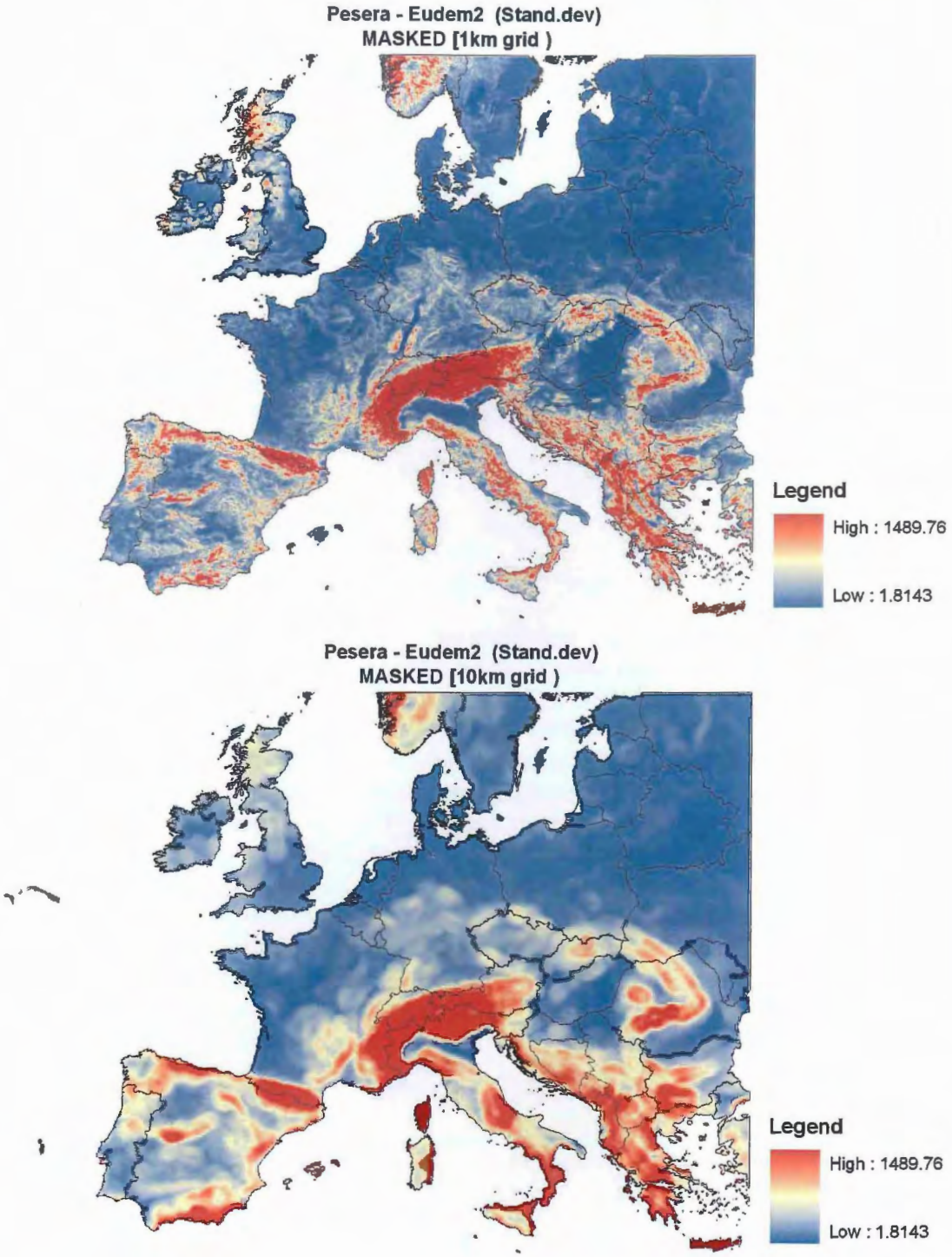

Figure 10

Spatial distribution of the average standard deviation of altitude calculated for two resolutions (1 km, above and 10 km, below).

In method B, the mean of the standard deviation of altitude was calculated for the 1 km DEM for all surrounding cells of one pixel (3X3 cell block). The relief intensity for the 10 km grid was calculated by averaging the standard deviation of altitude for all cells of 1km resolution grids in a 10km grid cell. The method delivers reasonable results when applying PESERA at 10 km grid. The comparison of the output results presented on the map and the histogram, suggests that the 10 km values are systematically lower. This is likely related to the lower spatial extent of the values for the different classes.

When comparing histograms of the output of PESERA (soil loss) based on the 1 and 10 km resolution DEM Figure 11 it is noted that the erosion rate estimates for 10 km grid are lower in all classes, except for the lowest class (that includes 0).

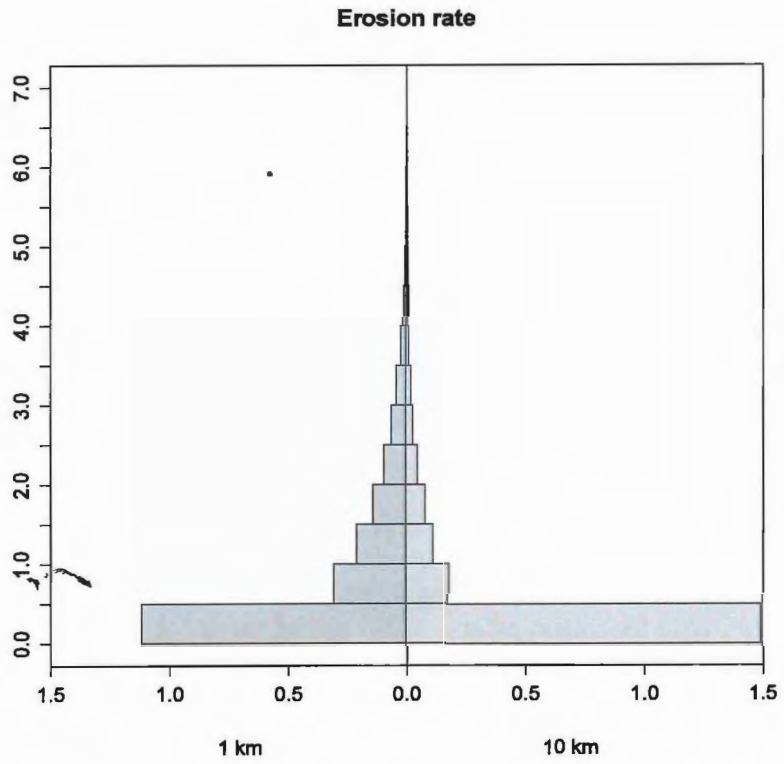

Figure 11

Histogram of PESERA output run of DEMs of 1 and 10 km resolution.

This is also visible in Figure 12 that shows the kappa statistics of the comparison between the PESERA runs on the two different DEMs. The values show a clear linear trend with no major deviations, except for the obvious deviation of the lower class values between the two approaches.

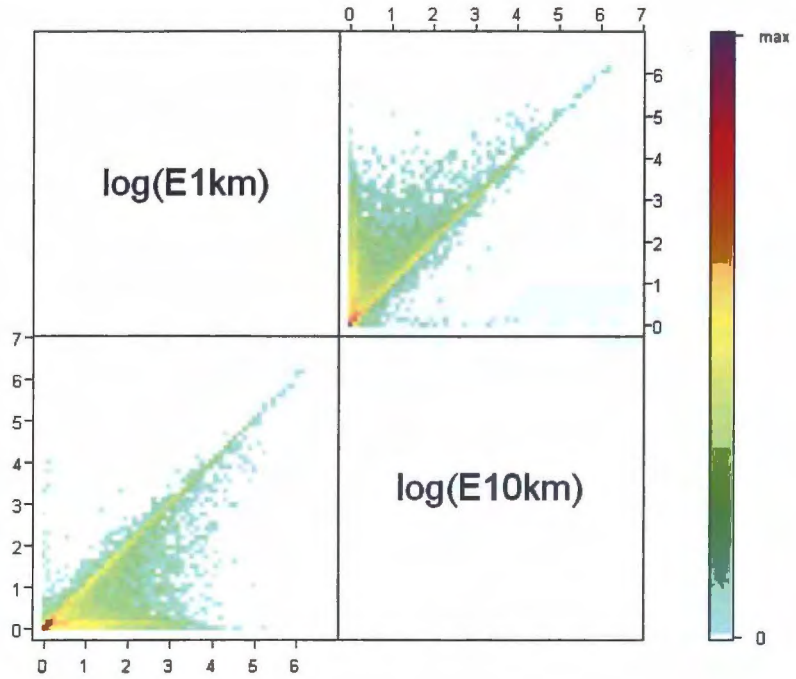

Figure 12

Kappa statistics diagram of PESERA output based on two resolution DEMs.

The PESERA output for the 1 and 10 km (Fig 13), is in agreement when comparing spatial patterns. The 10 km grid has generally lower estimates (systematic error). The difference is most noticed in the spatial extent of the erosion classes. While the pattern and the classes seem to agree, especially lower class values have less extent (area per output class).

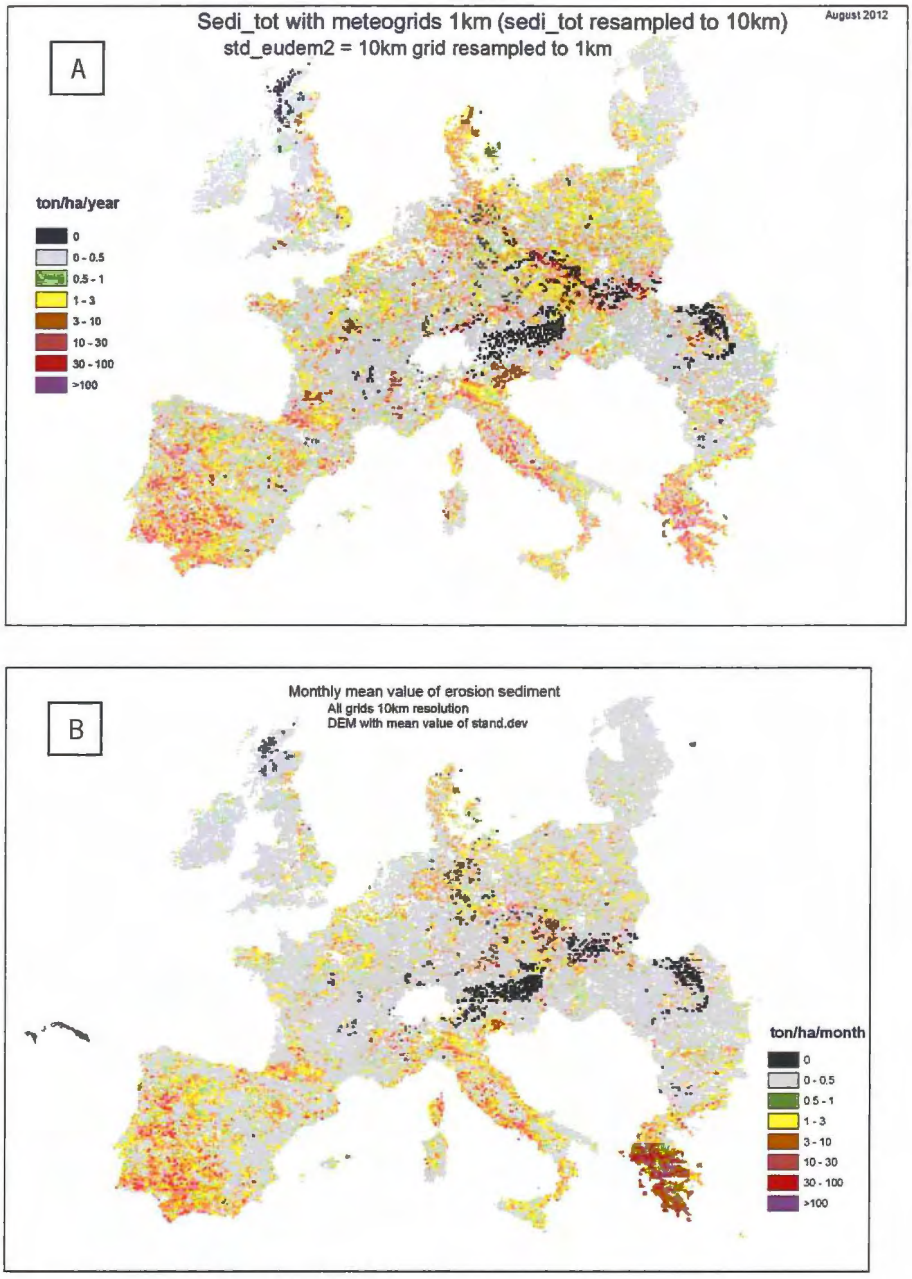

Figure 13:

PESERA estimated soil erosion (ton.ha-1.yr-1), annual output, based on 1 (A) and 10 km (B) DEM, compared at the 10 km resolution. Correlation: 0.45

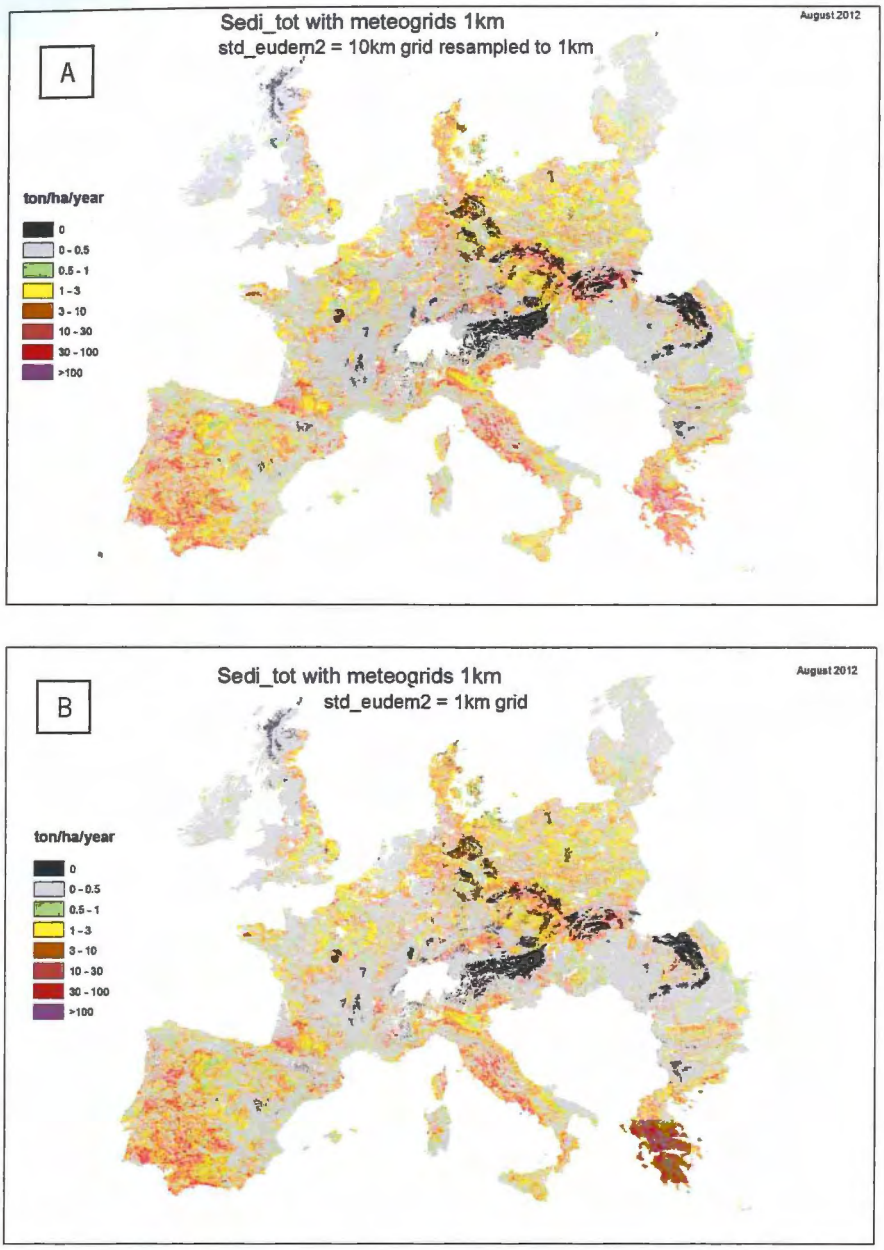

Figure 14

PESERA estimated soil erosion (ton.ha-1.yr-1), annual output, based on 1 and 10 km DEM, compared at the 1 km resolution. Correlation: 0.947

While creating the 1 and 10 km resolution output grids of erosion from the PESERA model, several transformations are done in the process. First, the 1 and 10 km grids are produced from the 90 m DEM by spatial aggregation to the two resolutions. Then, for the 10 km resolution run, there are two options: 1) aggregate all other data layers required to run PESERA to 10 km resolution grids and run the model at the 10 km resolution, or 2) overlay a 1 km mesh grid on the 10 km DEM and thereby creating a 1 km grid with 100 identical values for each block of 10x10 km's. The latter method was chosen, here as the assessment of the influence of the DEM resolution was the objective of the study. In that way the other data layers were kept at the base resolution, that was used for the original Pan-European erosion study, of 1 km. Within the 10x10 mesh grid different results are obtained for the 100 cells within the original 10 km grid, because the other data layers are still kept at 1 km resolution and have variable values in the 10x10 blocks. Aggregating back to the original 10 km resolution, therefore also involves a process

of averaging. When comparing the 10 km resolution run with the 1 km run, the data layers have been averaged to the 10 km resolution (Figure 13). The correlation is 0.45 for the PESERA output results based on the 10 km grid (run at 1 km resolution using the mesh grid overlay and results then averaged to 10 km), and the original 1 km run that was averaged to the 10 km resolution. The output results of PESERA using the 10 km DEM, but disaggregated to 1 km (using the 1 km mesh grid) and with 100 identical values for the 10x10 blocks, was also compared to the PESERA run at 1 km (all data layers), (Figure14). Then the correlation was much higher: 0.947.

Figure 15 a scatterplot of the 1 km versus 10 DEM resolution PESERA runs, shows that values are within the same range for predictions based on the two resolution scale DEMs. This is especially so for the lower sediment output predictions. In the higher sediment rates, values deviate more. The 10 km DEM based predictions of erosion appears higher than those of the 1 km DEM based predictions.

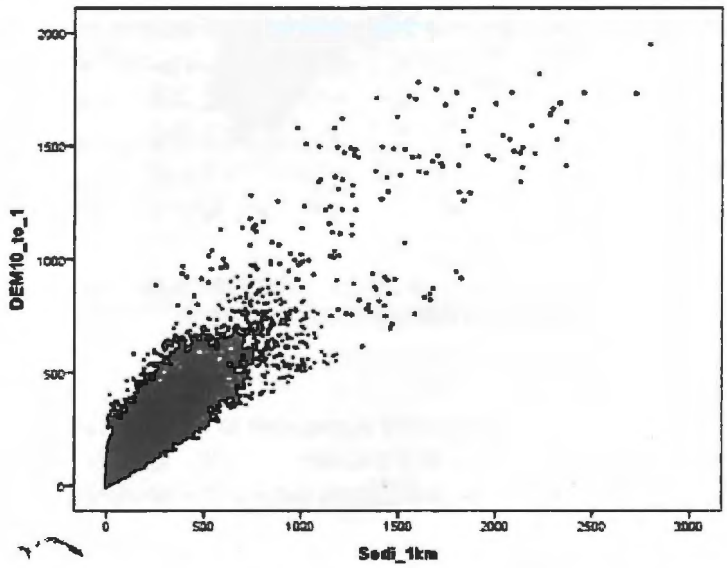

Figure 15

Scatterplot of sediment output (PESERA) for two resolution DEMs: 1 km (Sedi_1km) and 10 km (DEM10_to_1, subdivided in 1 km grid cells).

3.1.4 Conclusions

DEM compilation method

There are theoretical problems with the use of both methods for generation of a grid with the standard deviation of altitude. In both methods a systematical error is introduced. In method A, the (standard deviation of the) altitude systematically increases with grid cell size. Although this may be theoretically correct, as the internal variation of altitude will increase as the cells of the grid increases in size, yet for modelling erosion this means that all values systematically increase with DEM upscaling, the parameter is not scale independent for modelling erosion. Method B, the method where the higher resolution values (of standard deviation) are averaged in a 10 km grid block, produces systematically lower values. The output of the 10 km grid, produced using method B is closer, in pattern and intensity, to the erosion estimation based on the 1 km grid then when generated using method A and is therefore more adequate for use with PESERA.

PESERA output for different resolution DEMs (1-10 km, method B)

PESERA runs have been done using a 1km resolution and using a 10km resolution. For comparing the resulting erosion risk maps, two methods have been applied.

1. The 1km resolution outputs were aggregated to a 10km resolution. Next, a correlation between the aggregated 1km resolution map and the 10km PESERA output was calculated.
2. The 10km resolution outputs were disaggregated to a 1km resolution. Next, a correlation between the disaggregated 10km resolution map and the 1km PESERA output was calculated.

Both methods have disadvantages. in method (1), variation in the 1km map is averaged out. In method (2), the data map data are duplicated: the value for each 10km grid cell is used 100 times to calculate a correlation. The data duplication in method 2 leads to overestimation of the correlation and the results are therefore less reliable.

We conclude that differences between running PESERA at 1 and 10 km resolution DEMs does not have significant influence on the calculated sediment yield output. The aggregation and averaging does affect the output markedly. Several papers (e.g. Van Rompaey *et al.*, 2003; De Vente *et al.*, 2008) point to the sensitivity of PESERA for resolution of topography data, in effect DEM. Most of the authors claim or suggest that PESERA will perform better with resolutions higher (more detailed) than 1 km. Our comparison shows that PESERA output does not change when run on coarser resolution DEM data (10 km), when all other data are kept at the higher resolution (1 km).

3.1.5 Spatial patterns and scale sensitivity of IMAGE-USLE output

Method

The results of IMAGE-USLE simulations at 1km input resolution were aggregated to 10km by calculating a mean value for each 10km grid cell. Then, for 10% of the 10km resolution grid cells, simulation results for all model runs were extracted into a database and correlations between the simulation results were calculated. A sample of 10% was used for assessing scale sensitivity and consistency to avoid spatial auto-correlation.

Results

At 1km resolution, IMAGE-USLE predicts a pattern of erosion risks with low erosion risks in nature areas and high erosion risks in cropland areas, particularly in France and Southwest Spain. Although England is dominated by croplands, projected erosion risks are very low. Low erosion risks are also mainly found in mountain areas, that are characterized by natural or pasture land cover (Figure 16). The results at 10km resolution are very consistent with this, reflected by an agreement (r2) between the 1km and 10km model outputs of 0.84. The spatial patterns are very similar, but at 10km resolution the simulated erosion risks are lower and differences throughout the map are less pronounced (see histogram, Figure 17). Model outputs are very similar in mountain areas with large relief differences (Alps, Pyrenees, Carpathes) and in very flat areas (Netherlands). Especially in areas with a moderate relief the 10km model simulates a lower erosion risk. This is because in the 10km model the relief index is calculated using a threshold of elevation differences of 200m while in the 1km version differences up to 20 m are considered. This has been done to compensate for the larger elevation differences occurring at larger areas. Differences between the model output are, however, very small.

3.1.6 Conclusions

We conclude that the IMAGE-USLE is consistent across scales, and that better calibration of the relief index might further improve the consistency of the model across scales.

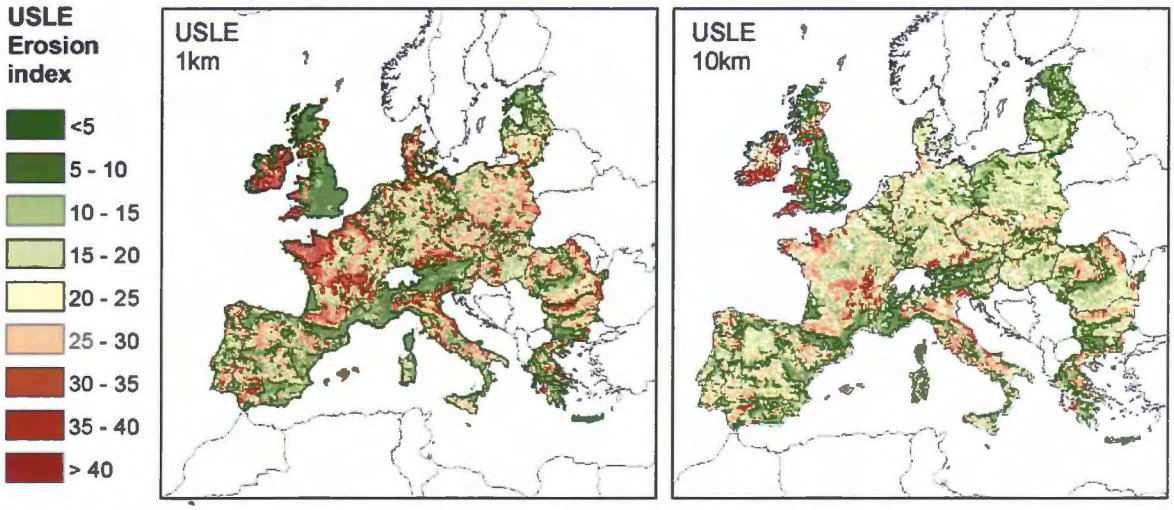

Figure 16

Comparison of IMAGE-USLE-1km and IMAGE-USLE-10km erosion risk outputs.

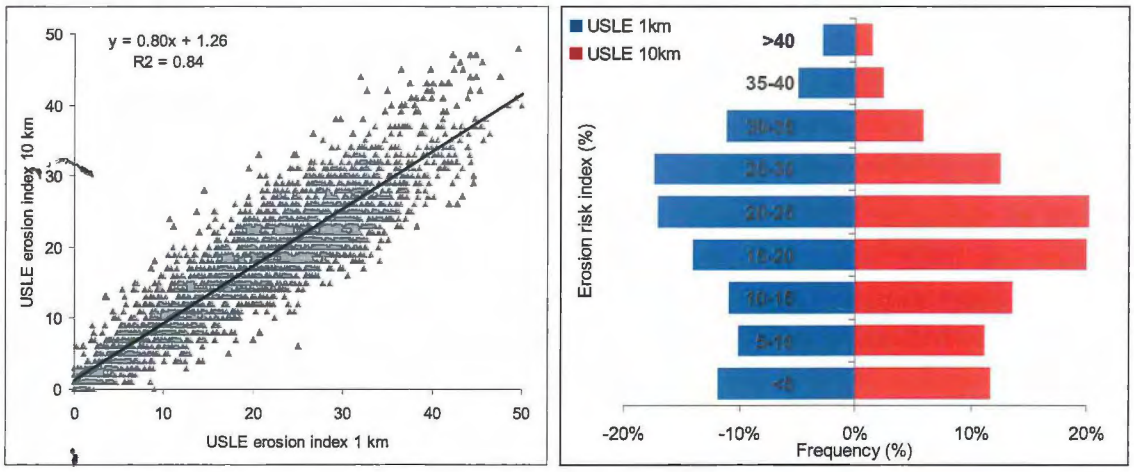

Figure 17

Scatter plots and histogrammes of IMAGE-USLE-1km and IMAGE-USLE-10km erosion risk outputs.

4 Evaluation of IMAGE-USLE and PESERA

4.1 Introduction

When substituting a sub-model within IMAGE, insight is needed in the differences between the outputs of the existing sub-model and the potential new version. Also, to be able to evaluate if applying PESERA at global scale within the IMAGE framework is expected to improve erosion risk simulations, we need to evaluate how PESERA behaves at a resolution feasible for global-scale simulations. We compared patterns of erosion risk simulated with both PESERA and the IMAGE-USLE and compared model outputs with existing global-scale data on several indicators of erosion and land degradation.
Because of the importance of DEM resolution for erosion modelling, and because other input data for the erosion models originate from coarser-resolution input, we focused on the effect of DEM resolution on the output of PESERA and IMAGE-USLE. For application at global scale, a resolution of 10 km or coarser is feasible. As PESERA was developed for a resolution of 1 km x 1 km, we simulated erosion risk with PESERA and with the IMAGE-USLE model, at a resolution of 1km and of 10km, resulting in four model runs. Simulations were done for the European Union excluding Sweden and Finland. A consistent dataset was used for all model runs. Model outputs were compared and evaluated with several datasets that provide an indication of spatial patterns and magnitude of erosion.

4.2 Methods

4.2.1 Models

The USLE-IMAGE is currently used at PBL for global-scale simulations of erosion risk to calculate an erosion index ranging from zero (no erosion risk) to 100 (high erosion risk) (Hootsmans *et al.*, 2001). The simplified formulation of the USLE in IMAGE, expresses erosion hazard as a function of terrain erodibility, rainfall erosivity and land use / cover index. The erosion index is arrived at through different steps.

Indices for texture (based on clay content and silt content), bulk density and soil depth are calculated using equations 4.1-4.3). For each grid cell, the maximum and second largest of these three indices were identified. The index is calculated as the average of these two indices:

$$I_{texture} = 100 * ((-0.005 * \text{Clay content}) + (0.005 * \text{Silt content}) + 0.5) \quad (3)$$

$$I_{bulkdensity} = \text{if(Bulkdensity} < 1.16\text{: 0, if(Bulkdensity} > 1.54\text{: 100 else((Bulkdensity} * 250) - 287.5))) \quad (4)$$

$$I_{depth} = 100 \text{ for soil depth} < 25\text{cm, 90 for soil depth} < 50 \text{ cm, 60 for soil depth} < 100 \text{ cm, 25 for soil depth} < 150 \text{ cm, else zero} \quad (5)$$

The relief index is set at 100 when elevation range within a grid cell exceeds 2%. Below 2%, the relief index is proportional to the elevation range. All elevation ranges larger than 2% are considered to result in maximum erosion risk.

The terrain index (VUI) is calculated as the average of the soil index and relief index.
Rainfall erosivity (REI) is calculated using maximum monthly rainfall (mm) per rainday. It is assumed to be proportional to the erosivity between 2 mm/day and 20 mm/day. Below 2 mm/day, REI is set at zero and above 20mm, REI is 100.
Hootsmans *et al.* (2001) specify global indices for the amount of protection provided by different crop types. These are multiplied with cover percentages for each crop into a Land Use Index (LUI).
Finally, the erosion risk index is calculated as

(VUI + REI) / 2) * LUI (6)

4.2.2 Input Data

Both the IMAGE-USLE and PESERA approach need input data on soil, land use /cover, elevation and weather. Basically, the data from standard PESERA runs were used here (Table 4), but some adaptations were necessary, as described in Table 4.

Table 4
Inputs and edits of data for model comparison.

	Data sources (resolution)	Adaptations at 1km resolution	Adaptations at 10km resolution
Weather	MARS (from PESERA datasets; point dataset, 50km grid	Interpolation to 1km resolution (original PESERA input dataset)	Mean of original PESERA inputs aggregated over 10 km block
Land use	Corine land cover (100m)	Reclassified to PESERA land cover classes. Aggregated to 1km resolution by calculating fractional cover for all land cover and crop types	Reclassified to PESERA land cover classes. Aggregated to 10km resolution by calculating fractional cover for all land cover and crop types
Elevation	SRTM (90m)	Aggregated to 1 km resolution (see Chapter 3)	Aggregated to 10 km resolution (see Chapter 3)
Soil	European Soil Geographical Database (scale 1: 1 million)	Clay, silt, sand content, Erodibility, depth, crusting, bulk density extracted and converted to 1km resolution raster	Mean over 10x10 km block

4.2.3 Map comparisons, assessment of credibility of results

To analyse model scale sensitivity and the consistency between PESERA and IMAGE-USLE in calculating erosion risk, the same datasets were used. First, the results of IMAGE-USLE and PESERA simulations at 1km input resolution were aggregated to 10km by calculating a mean value for each 10km grid cell. Then, for 10% of the 10km resolution grid cells, simulation results for all four model runs were extracted into a database and correlations between the simulation results were calculated. A sample of 10% was used for assessing scale sensitivity and consistency to avoid spatial autocorrelation.
To demonstrate the impact of different behaviour of the model parameters, we selected four small sample areas in Spain, UK, Greece and Austria (Figure 18a), representing areas with large elevation differences (Greece, Austria) versus areas with small elevation differences (UK, Spain) and areas with high erosion risk (Spain, Greece) versus areas low erosion risk (UK, Austria). For these sample areas, the differences in outputs between the models are analysed in more detail here.

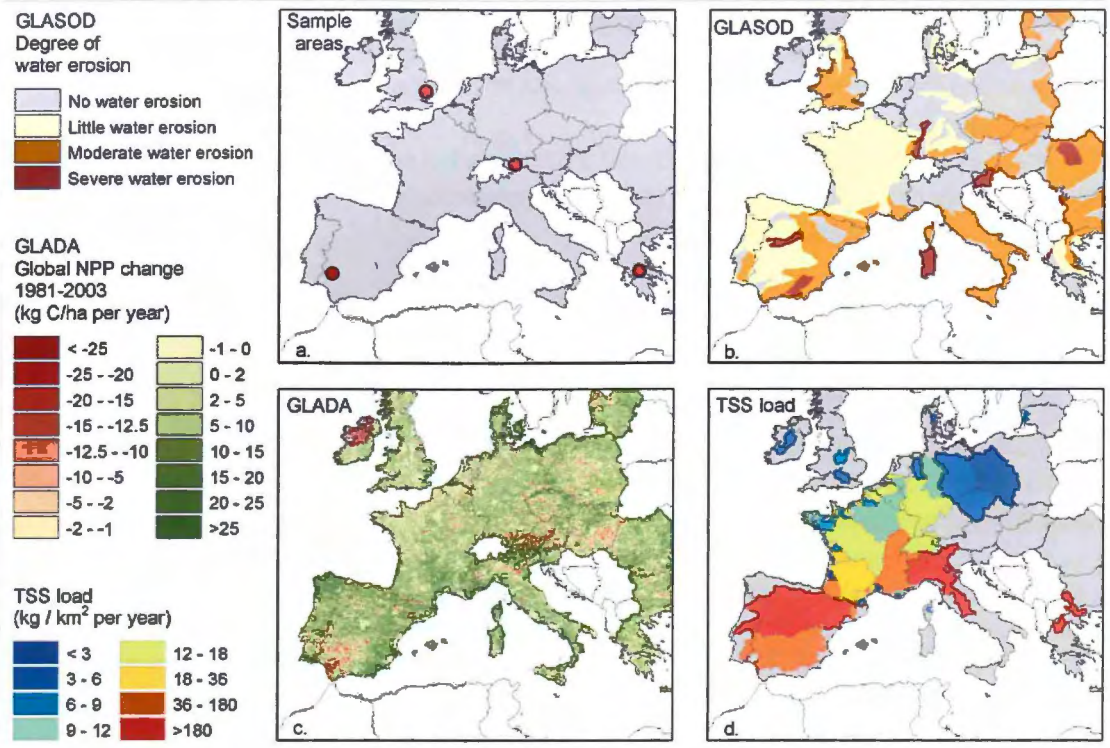

Figure 18

a. Sample areas; b. Degree of water erosion as indicated by GLASOD; c. Changes in NPP from GLADA; d. Total suspended sediment load (TSS) from EEA observations.

To evaluate PESERA and IMAGE-USLE simulations at 1km and 10km resolution, model outputs were compared with several datasets that provide an indication of spatial patterns and amount of erosion throughout Europe. For a proper validation, a dataset is needed that provides quantitative data of actual observed data on sheet erosion throughout Europe. In the absence of such a dataset, the following several proxies were used to assess the credibility of the model outputs:

- GLASOD (Oldeman, *et al.* 1991)
- GLADA (Bai, *et al.*, 2008); and
- a dataset on total suspended sediment (TSS) delivered at the mouth of several drainage basins throughout Europe (EEA, 1998)

GLASOD

GLASOD is an inventory of expert judgements on the extent and severity of erosion and degradation worldwide (Figure 4.1b). Based on physiographic units, a large and diverse group of experts rated the extent (percentage of the polygon affected) and degree (strongly, moderately or slightly degraded) of past erosion and degradation (Oldeman *et al.*, 1991). Several types of erosion are evaluated: namely sheet erosion, rill and gully erosion, wind erosion, loss of nutrients, salinization, acidification, pollution, compaction, sealing, crusting, waterlogging and subsidence. The GLASOD represents the state of degradation that has occurred until 1990, thus over 20 years ago. The subjectivity of the map and the coarse spatial resolution is another weakness. When comparing the simulation results with GLASOD, we hypothesize that areas with a high extent or degree of sheet erosion corresponds with areas with high simulated erosion risks.

GLADA

GLADA provides an indication of more recent, inferred degradation than GLASOD. Based on remote sensing images from 1981-2003, areas with a change in NDVI and associated change in Net Primary Productivity (NPP) are identified (Figure 18c). Areas with a decreased NPP over the timeframe assessed are assumed to have been degrading over the observed period, with the strength of the NPP decrease being taken as a measure of the severity of degradation (Bai *et al.*, 2008). Advantage of GLADA is that the map provides an up-to date overview of the status degradation, with a global coverage and a high spatial resolution. GLADA is an objective map, in the sense that it is reproducible and verifiable. Furthermore, GLADA indicates trends in both directions, decline and increase of NPP, as a proxy for land degradation and improvement respectively. However, GLADA rather indicates estimates the effects of degradation (assumed to correspond with a NDVI decrease) in general; different possible causes for degradation cannot be distinguished. We do expect that areas with a higher projected erosion risk in our simulations are more likely to be degraded and therefore expect an overlap between degraded areas in GLADA and areas with a high erosion risk.

Total Suspended Sediment delivery

The European Environmental Assessment Agency (EEA) provides data on total suspended sediment (TSS) output at basin scale throughout Europe in 2000 (ton/year) (EEA, 1998), (Figure 18d).
We recalculated this into TSS delivery per km^2 over each river basin and compared the numbers with average (and ranges of) erosion risk simulated in each basin. Also several basin characteristics including elevation range, percentages cover by certain crops and distribution of soil texture classes were considered here. With this dataset, several statistics were calculated to relate the erosion outputs to the TSS load. We expect that a higher TSS delivery is associated with a higher erosion risk. The dataset however provides a lumped erosion risk for each river basin (Figure 18d) and therefore does not account for spatial patterns of erosion and sedimentation within a basin.

Although these datasets differ in the indicators mapped and all three maps *actually do not match the outputs of the erosion models that represent sheet erosion risk*, one would expect some correlation with the erosion risk simulations. To quantify the match, several parametric and non-parametric statistics were used, depending on the data.

4.3 Results: Model comparison and scale sensitivity

4.3.1 Comparison IMAGE-USLE/PESERA

USLE and PESERA result in different patterns of erosion risk throughout Europe. While the USLE estimates high erosion risks in croplands and slightly sloping areas and intermediate risks in Mediterranean areas, PESERA estimates high erosion risks throughout the Mediterranean areas and intermediate risk in the rolling cropland areas of central Europe. Correlations between PESERA and USLE are very low (Table 5) and the frequency distribution of erosion risk is completely different (Figure 19).

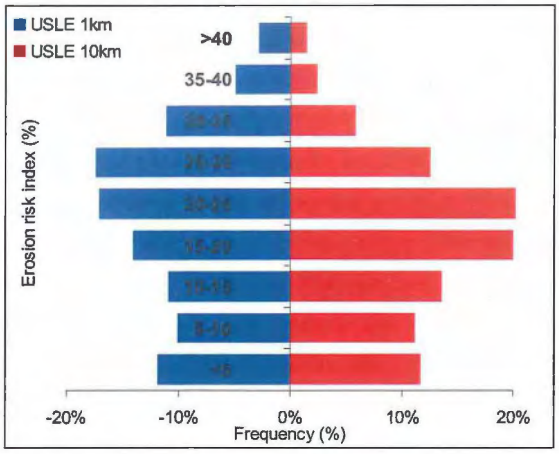

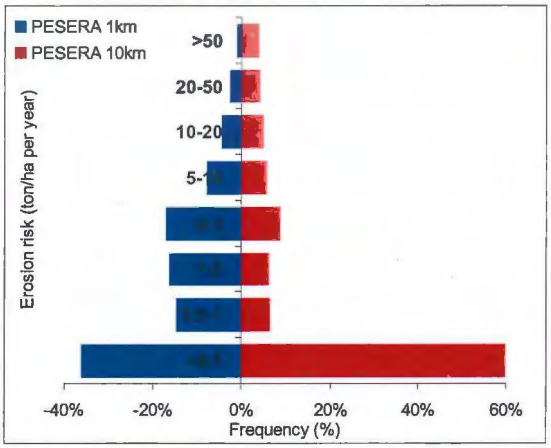

Figure 19

Comparison of histogrammes PESERA/IMAGE-USLE.

Table 5

Correlation between Pesera and USLE projections at 1km and 10km resolution.

	PESERA		IMAGE-USLE	
	1km	**10km**	**1km**	**10km**
PESERA-1km	1.00			
PESERA-10km	0.58	1.00		
IMAGE-USLE-1km	0.02	0.06	1.00	
IMAGE-USLE-10km	0.06	0.09	0.92	1.00

Several reasons can be found for these differences. First, there are differences in effect of soil sensitivity to erosion. While in the USLE the sensitivity to the soil for erosion is based on clay content, silt content and bulk density, in PESERA physico-chemical stability is accounted for in determining the erosion sensitivity. Especially in the Northwest European sand area, this results in higher erosion sensitivity in PESERA. In the four sample areas, the sensitivity to erosion matches those of the study areas.

Second, the models differ in how they simulate the effect of relief on erosion. In IMAGE-USLE, elevation differences within a grid cell of >2% are considered to result in a maximum erosion risk due to relief, while below 2% the erosion risk is linearly related to the elevation difference. In PESERA, the relief is not cut-off beyond a threshold, but the complete elevation range (standard deviation, see section 2.2.4) is used to calculate sediment transport. Consequently, small elevation differences have relatively less impact on the erosion risk than in IMAGE-USLE, while more differences in erosion risk are simulated in mountainous or hilly areas. The relatively low erosion risks in flat areas in PESERA can be most clearly observed in the Netherlands and the Baltic Countries. In Greece, Spain and Italy the effect of large elevation differences in different model simulations can be observed.

Third, the impact of precipitation is simulated differently. IMAGE-USLE works with the maximum monthly rain intensity within a year. This is, for example, high in Ireland and France and is partly causing the high erosion risks in these areas. Maximum rain intensity is low in the Mediterranean, being partly causing the lower, simulated erosion risk simulations. In PESERA however, the temporal distribution of precipitation throughout the year is taken into account; this is reflected in the four examples.

Finally, although IMAGE-USLE and PESERA use a similar land cover and land use classification, the parameterization of the effect of land use and land cover is different (Table 6). Particularly in areas with much grassland cover, this can be a reason for the relatively lower erosion risks in PESERA compared with the IMAGE-USLE simulations. Under European conditions, the parameterization of grassland in PESERA might be more realistic while the parameterization in IMAGE-USLE might be more representative for global conditions.

Table 6

Comparison of land use / land cover effect on erosion in IMAGE-USLE and PESERA.

Land use / cover	IMAGE-USLE index (converted to 100 = full protection, zero = no protection)	PESERA cover % range	PESERA months with cover
Grass	60	100	12
Temperate cereals	35	8-96	10
Maize	5	17-94	5
Pulses	35	19-98	4
Root crops	15	11-99	6
Oil crops	20	13-95	5
Extensive grassland	60	100	12
Scrubs	85	30	12
Other	100	100	12

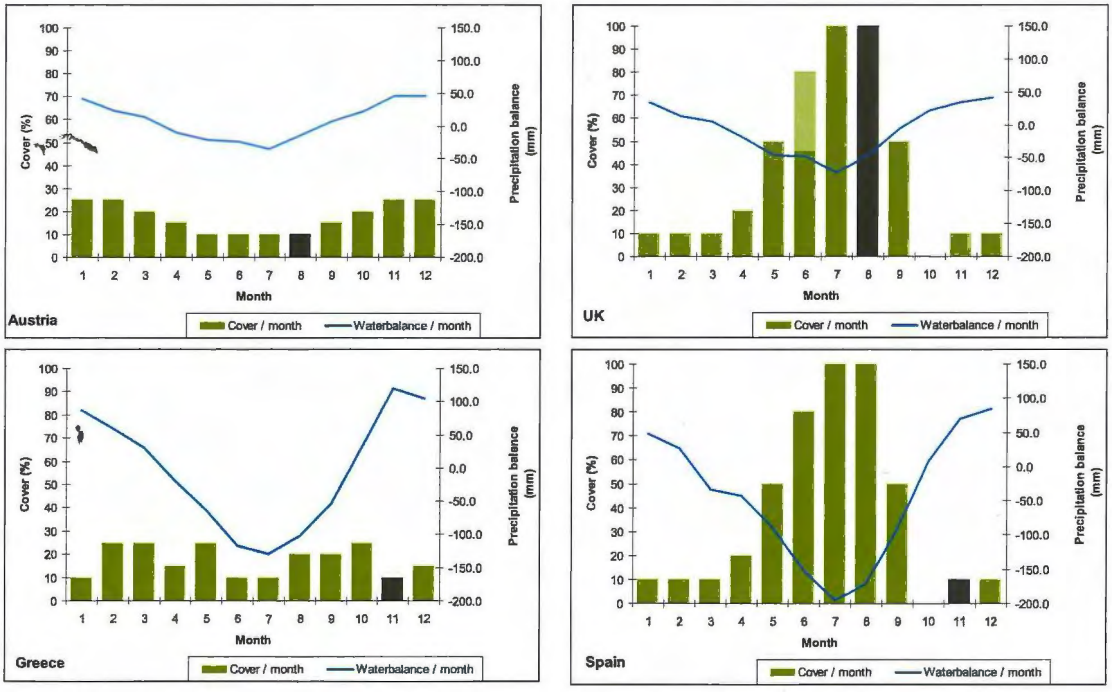

Figure 20

Comparison of PESERA inputs in four sample areas. Bars (left axis) are the vegetation cover percentage, line (right axis) is the precipitation surplus / deficit. The dark green bar indicates the month with the highest precipitation intensity.

Table 7

Comparison of USLE and PESERA inputs and outputs in selected sample areas in four countries.

Parameter	UK	Greece	Austria	Spain
IMAGE-USLE				
Erosion risk (0-100)	1.02	2.52	6.26	18.94
Land use index (0-100)	97.43	99.97	88.38	67.53
Rain intensity index (0-100)	11.70	53.00	28.00	35.40
Landscape vulnerability (0-100)	66.00	89.00	82.91	81.75
PESERA				
Erosion risk (ton.km^2 per year)	0.22	324.66	0.04	113.54
Erodibility (0=low, 5=high)	2.15	2.84	2.95	4.9
Stdev DEM (m)	0.50	225.11	435.26	15.67

Sample areas

In the sample area in Austria, IMAGE-USLE estimates a high landscape vulnerability which is reflected in PESERA by the high elevation differences and intermediate erodibility. IMAGE-USLE estimates a lower land use index, indicating low protection by the vegetation cover. This matches the low cover percentages in PESERA. The rain intensity is moderate and constant through the year. Also in the IMAGE-USLE the rain erodibility is low. Consequently, both models simulate a low erosion risk.

In the UK sample area, both models indicate a low vulnerability of the landscape and a low rain intensity. The land use index in the IMAGE-USLE (in agricultural land) is parameterized in such a way that it matches the interaction between rain intensity and cover through the year as used in PESERA the highest rain intensity is found in a month with a very high vegetation cover (Figure 20).

Greece has variable topography and a precipitation surplus with high rain intensity in a month with a low cover percentage. Erosion predictions for Greece resulted in high erosion, although the sensitivity of the soils to erosion is not too extreme. In this area the effect of rain and landscape match well with the IMAGE-USLE, but the USLE estimates a completely different effect of vegetation (high index). Although there is a year-round vegetation cover, the fractional amount of cover is very low, particularly in the month with the highest rain intensity.

In the Spain sample area, both models indicate highly sensitive landscapes. In PESERA, the sample area has a precipitation surplus with high rain intensity in a month with a low cover percentage, resulting in high erosion. The land cover parameterization in agricultural landscapes in the USLE does capture this well (lowest land use index). Also, the high rain intensity is captured relatively well in the USLE.

4.4 Results: Credibility of erosion risk simulations

4.4.1 GLASOD

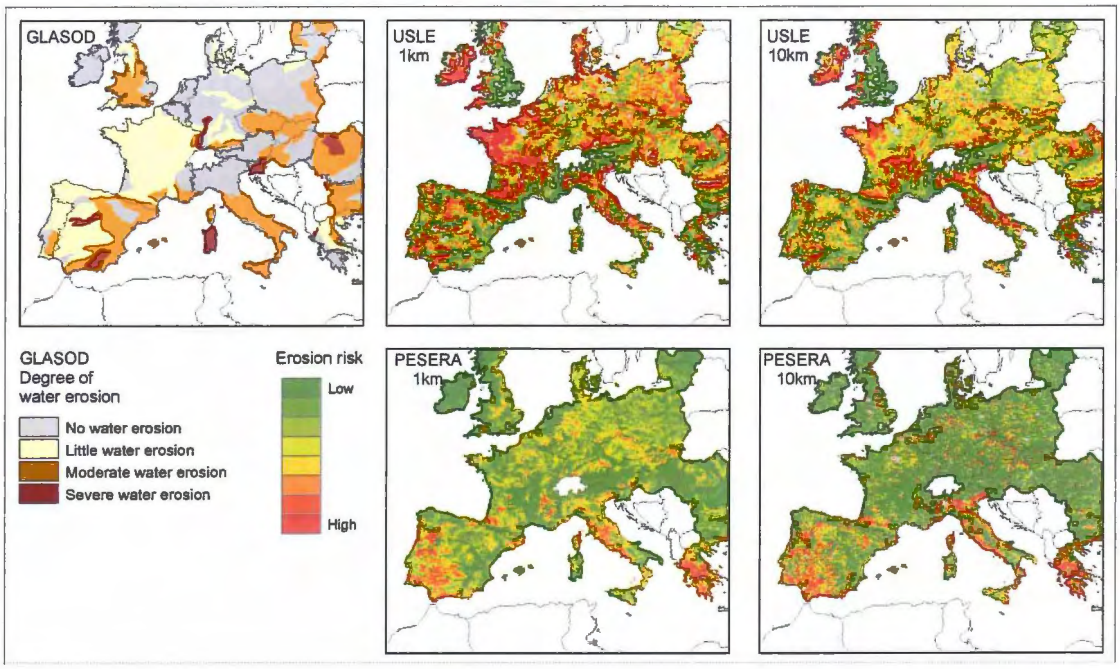

Figure 21

Comparison of GLASOD and erosion model outputs.

When visually comparing IMAGE-USLE outputs with GLASOD, in Central Europe, there seems to be some overlap between patterns of simulated erosion risks and expert based patterns of sheet erosion degree. Areas with moderate water erosion in GLASOD in Bulgaria, Romania, Czech Republic, Slovakia and France overlap with areas with a higher erosion risk in the USLE simulations. In the Mediterranean, the map patterns almost contradict.

For PESERA, only in the Czech Republic, Poland and Germany there is some overlap between areas with a higher degree of erosion in GLASOD and more erosion risk in PESERA. This applies both for the 10km and the 1km outputs of PESERA.

Table 8 shows the results of a non-parametric rank test (Jonckheere-Terpstra test, JT test) to assess if the erosion risk model output increases through the erosion degree classes of GLASOD. For PESERA at 1km and 10km resolution, the positive JT statistics indicate that there is indeed a trend of increasing erosion risk within classes of increasing GLASOD erosion degree. For the IMAGE-USLE, a reverse trend is observed, both at 1 and 10 km resolution (sign <0.05).

The extent of sheet erosion in GLASOD was compared with the areas of high erosion risk in the model output. For this, erosion risk in the model output was classified for the IMAGE-USLE following the classes given by Hootsmans *et al.* (2001). Indices < 15 are interpreted as no or low erosion risk, 15-30 as moderate erosion risk, 30-45 as high erosion risk and >45 as very high erosion risk. The PESERA outputs were classified into four classes using similar percentual class sizes as for the USLE. The classes were compared with GLASOD using a Chi squared test, assuming that classes of higher erosion risk in the model output should overlap with a larger extent of erosion in GLASOD. The high and significant (<0.05) Chi square values (Table 8) show that the classes of GLASOD erosion extent are indeed related to the classes of erosion risks of all model outputs. A check of the cross-tables indicated

that, for both models, indeed GLASOD classes with a small extent of erosion have larger areas with little erosion risk, while GLASOD classes with a large extent of erosion have larger areas with high erosion risk. The low V values (Table 8), around 0.10, indicate however that the effects are weak.

Table 8

Comparison of model outputs with indicators for erosion risk.

Model	IMAGE	USLE		PESERA
	1km	10km	1km	10km
standardized JT statistic – GLASOD degree	-5.493	-2.604	4.706	2.289
ChiSquare – GLASOD extent	109.57	73.1	100.88	91.36
Cramers V – GLASOD extent	0.109	0.089	0.095	0.096
Spearman's correlation coefficient vs.GLADA NPP change (r)	-0.2	-0.16	0.01^{ns}	-0.03
Correlation (r) ln-transformend average erosion @ basin level with TSS data				
Whole Europe	-0.147^{ns}	-0.098^{ns}	0.238	0.34
Northern Europe	0.521	0.559	-0.160	-0.248
Southern Europe	-0.315	-0.282	0.327	0.469

4.4.2 GLADA

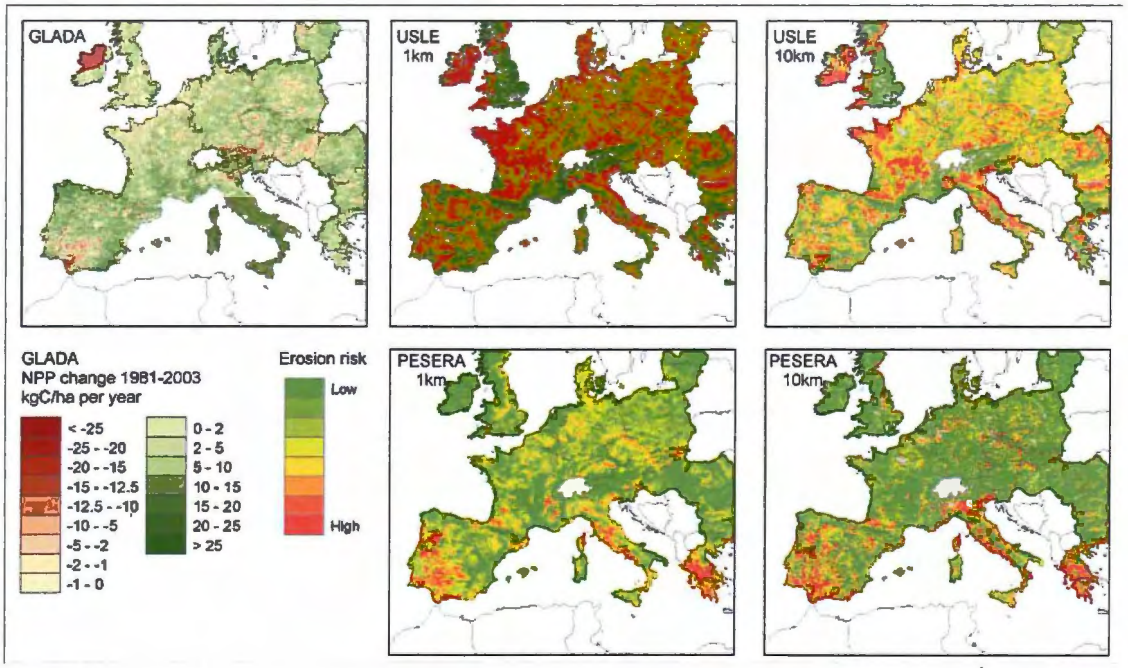

Figure 22

Comparison of GLADA and erosion model outputs.

Visually, higher USLE-simulated erosion risks in Southwest Spain, the Po plain in northern Italy and southern Germany match areas of NDVI loss in GLADA, while areas of low erosion risks simulated with the IMAGE-USLE in the French and Italian Alps, the Pyrennees and Carpathes match areas of NPP increase in GLADA.

For PESERA, at both 1km and 10km resolution, in Spain and Portugal the patterns of GLADA and the model output seem to overlap well, both for the areas with high erosion risk and the areas with low erosion risk. Also in Italy and France the patterns of erosion risk and NPP change seem to match well.

The low erosion risks simulated in Hungary and the Alps contrast with the large NPP losses observed in GLADA. This could be caused by the fact that GLADA observes NPP losses in several mountain areas due to other causes than sheet erosion while PESERA simulates low erosion risks due to the low erodibility of the rocks and/or to the vegetation cover.

According to the statistical analysis, however, IMAGE-USLE model outputs show a significant, but weak negative correlation with the NPP change (Spearman's r), indicating that higher simulated erosion risks match with areas with a larger NPP loss. For the PESERA model outputs correlations are even weaker (Table 8).

4.4.3 Total Suspended Sediment load data

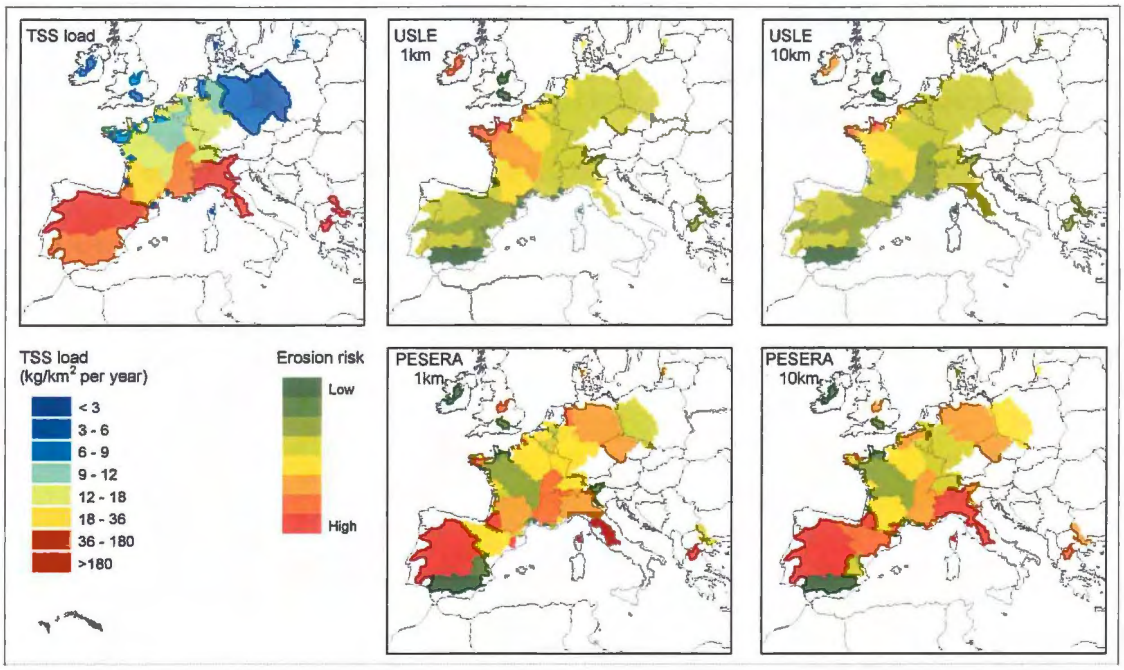

Figure 23

Comparison of TSS loads and erosion model outputs.

The TSS load per km^2 produced in drainage basins is high in the Mediterranean, intermediate in France and Germany and low in northern Europe (Figure 4.10). In comparison, this, IMAGE-USLE shows the reverse patterns in southern Europe, while in the northwestern half of France and in northern Europe the patterns seem to overlap. The patterns of PESERA outputs broadly match the TSS patterns in southern Europe and look contrary in the northwestern half of France and in northern Europe.

If the model outputs are averaged per basin and compared with the TSS load, we observed that all over Europe, the IMAGE-USLE outputs showed no significant correlation with the TSS loads while the PESERA outputs showed a better correlation if the model outputs were first ln-transformed. Non-transformed data did not show a significant or meaningful correlation with the TSS load data. When the dataset is split-up in northern Europe and southern Europe, IMAGE-USLE-outputs showed a significant positive correlation with the TSS loads in northern Europe, while in southern Europe correlations were negative. PESERA showed opposite patterns: Positive correlations, as expected, in southern Europe and negative correlations in northern Europe.

For a more detailed analysis of the PESERA outputs, Sediment Delivery Ratios (SDR) were calculated using the PESERA outputs and the observed TSS loads. SDR's are defined as the amount of erosion simulated with the PESERA model, divided by the observed TSS loads. An SDR < 1 means that total erosion simulated with PESERA is lower than the amount of sediment delivered at the mouth of the basin. This can indicate that in these basins sediment delivery to the river is dominated by processes not described in PESERA, e.g. gully erosion or mass movements. An SDR > 1 indicates that PESERA simulates more erosion than loads reach the mouth of the basin. This can indicate that erosion is redistributed within the basin and does not reach the stream system.

SDR's are calculated to range between 0.012 and 165 for the PESERA-1km outputs and between 0.015 and 720 for PESERA-10km outputs. Both PESERA-1km and PESERA-10km tends to underestimate erosion in basins with a high TSS load and overestimate erosion in basins with a low TSS load (Figure 24). Underestimations of the erosion by PESERA are also found by several authors in several case studies.

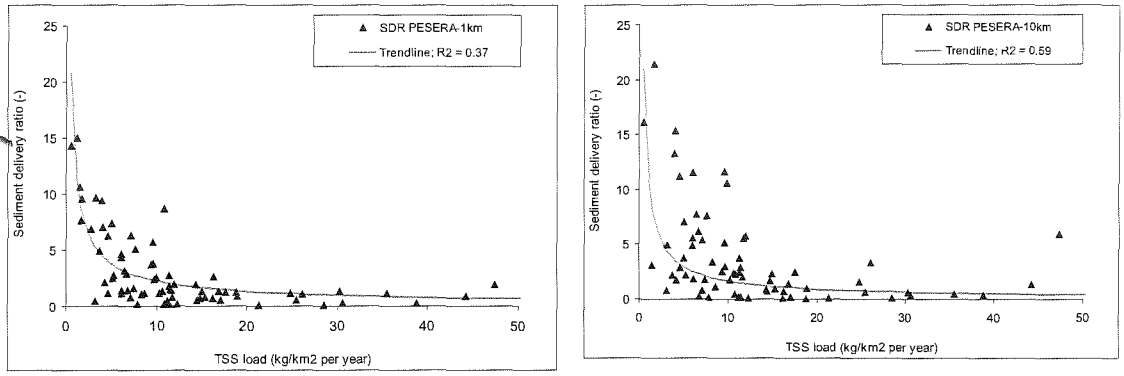

Figure 24

Sediment Delivery Ratio (SDR) of PESERA simulations compared with total suspended sediment load (e.g. (Van Rompaey et al., 2003, De Vente et al., 2008).

For both PESERA-1km and PESERA-10km, basins where PESERA overestimates erosion (SDR>1; probably a lot of re-sedimentation within the basin) are characterized by (t-test, $p<0.05$) a significantly lower elevation, higher clay content and higher silt content than the basins where PESERA underestimates erosion.

A basin with a lower average elevation is generally less hilly and has less steep slopes. In such a basin, re-sedimentation is more likely to occur. Soils with a higher silt content are more sensitive to erosion.

This effect might be exaggerated in PESERA, causing an overestimation of the erosion. Higher clay contents can have two effects: lower infiltration rate and higher crusting risk, resulting in higher runoff, and their effects may be poorly parameterized in PESERA. On the other hand, higher clay contents also stabilize the soil.

4.5 Conclusions

The effects of vegetation cover and relief are interpreted differently by the models. Considering the interaction between timing of vegetation cover and rain intensity through the year in PESERA versus using values aggregated over a year resulted in large differences especially in areas with highly variable vegetation and rain over time.

For a solid validation of the erosion risk simulations with PESERA and IMAGE-USLE, data on water-induced sheet erosion over the past decades throughout Europe are needed. Because of lack of such data, we compared the model results with several maps that provide an indicator of the amount of erosion and degradation. Although comparing the output of a model that simulates long-term average erosion risk with a map of an indicator of past or current degradation status cannot be expected to fully align as we compare different variables, some correlation between the model outputs and the degradation indicators might be expected, underpinning the credibility of the models. In the end, the "sensitivity to erosion" as estimated with the models may compare to the status (GLASOD) and rate of erosion (GLADA, TTS).

Compared with GLASOD erosions status, PESERA calculated erosion risk is higher in areas where more severe erosion is observed until 1990, as is expected, while IMAGE-USLE simulates the reverse pattern. Both PESERA and IMAGE-USLE predict larger areas of high erosion risk in areas where GLASOD indicates a large extent of erosion status. The statistical trends are however not strong, and because of the very large polygons used in GLASOD the results of the comparison are very coarse, there is a large chance that any overlap is coincidential (Shown by the low Cramer's V values).

IMAGE-USLE outputs are negatively correlated with those of GLADA, so areas with an NDVI decrease due to degradation are facing higher erosion risk. PESERA simulates a reverse pattern. *This could, however, mean that the degradation observed in GLADA is caused by other processes than water-induced erosion.*

Compared to the TSS dataset, IMAGE-USLE outputs show a comparable pattern in northern Europe while PESERA outputs show a reasonable correlation with TSS loads in southern Europe. Also, all over Europe PESERA has a somewhat better correlation with the TSS dataset. PESERA does however underestimate erosion. The underestimation is larger in basins with a higher TSS load.

5 Options for PESERA and IMAGE/LPJ

5.1 Introduction

Within the global change integrated assessment framework IMAGE, water erosion is simulated with a simplified version of the IMAGE-USLE (as described in section 4.2). Currently, the vegetation growth module and water module of the IMAGE framework is being replaced by the global dynamic vegetation models LPJ and LPJmL.

When *adding* PESERA to the IMAGE framework, PESERA should be run using inputs or outputs from scenarios simulated with IMAGE or IMAGE/LPJ. In section 5.2 we describe the data requirements for PESERA in more detail and evaluate the use of IMAGE / LPJ inputs and outputs as alternatives. Then, in section 5.3 the application of PESERA in feedback with IMAGE / LPJ to simulate impacts of erosion on crop production is evaluated. Section 5.4 provides a script for running PESERA using IMAGE or LPJ inputs and outputs and evaluates the steps needed for this.

5.2 Data match between PESERA and IMAGE/LPJ

Tables 9-11 describe the input data for a standard PESERA run for the European union, and data used or generated by IMAGE and LPJ that could be used as an alternative. Table 9 describes weather and water data, Table 10 describes soil and topography data and table 11 describes land cover and use data.

Weather

Both IMAGE and LPJ use and simulate monthly weather data. The models are based on a global dataset of climate data with a 50km resolution. Algorithms are available for downscaling monthly weather data to daily data, enabling calculation of the temperature range and variation in precipitation needed for PESERA. Thus, technically speaking, weather data from the IMAGE framework suffice for running PESERA.

Alternatively, instead of fully running PESERA using IMAGE or LPJ data, runoff as simulated with IMAGE or LPJ could be used directly as input to simulate soil loss with PESERA. Both IMAGE and LPJ calculate runoff with a tipping bucket model that is quite comparable with the approach used in PESERA. Drawback of directly using the runoff simulated by IMAGE and LPJ is that both IMAGE and LPJ use a poor representation of limitations to infiltration due to depth and crusting. In both IMAGE and LPJ, runoff thus probably is underestimated (Sitch *et al.* 2003), making the IMAGE / LPJ runoff simulations probably unsuitable for simulating water-induced erosion.

Soil and topography data

Both in IMAGE and in LPJ, highly generalized soil data are used that are not sufficient for running PESERA (Table 10). For global-scale applications, additional soil data are needed to run PESERA. The PESERA input parameters are derived from the Soil Geographical Database of Eurasia (SGDE) through a set of pedo-transfer rules. To derive these input parameters from a global-scale database, such as the Harmonized World Soil Database (HWSD), pedo-transfer rules need to be developed to fit such a database. Input data needed for this are however incomplete in the HWSD, especially indicators for soil depth.

With respect to topography, both IMAGE and LPJ use a map indicating areas considered unsuitable for crop production due to relief. To run PESERA on global scale, additional data on elevation is needed. Several global-scale DEMs are available that would suffice for this goal, including the SRTM 90m resolution DEM and the GTOPO30 1km resolution DEM.

Table 9

Weather / Water data comparison.

PESERA inputs **Description, unit**	**Model boundary conditions**	**Closest Alternative from IMAGE inputs / outputs**	**Closest Alternative from LPJ / LPJmL inputs / outputs**
Mean monthly rainfall (mm mo^{-1})	0-300	Monthly precipitation (mm yr^{-1})	Monthly precipitation (mm mo^{-1})
Mean monthly rainfall per rain day, by month (mm d^{-1})	0-50	Monthly number of wet days (yr^{-1})	Stochastic downscaling of monthly precipitation to daily precipitation
Coefficient of variation of rainfall per rain day (by month, computed for rain days only)	-		
Mean monthly temperature, corrected for altitude (°C)	-20-21	Mean monthly temperature (°C)	
Temperature range (Mean daily max -mean daily min) (°C)	2.4-18.4		
Mean monthly potential evapotranspiration PET (mm mo^{-1})	0-300	Precipitation surplus (mm yr^{-1}) PET (mm yr^{-1}).	Monthly transpiration (mm mo^{-1}) Monthly soil evaporation (mm mo^{-1})

Table 10

Comparison of soil and topography data needed for running PESERA, IMAGE and LPJ(mL) models.

PESERA inputs **Description, unit**	**Model boundary conditions**	**Closest Alternative from IMAGE inputs / outputs**	**Closest Alternative from LPJ / LPJmL inputs / outputs**
Erodibility	1-5	Reduction factor of potential production (-) based on: - Fertility (5 classes) - Salinity (2 classes) - Rooting depth limitations (4 classes) - Acidity (3 classes) - Drainage (2 classes) These limitations are specified in n classes for FAO main soil types. (Leemans 1994)	9 texture classes, derived from the FAO soil map of the world. Per texture class are specified: o Percolation rate; o Water holding capacity; Texture Classes are: Coarse; Medium; Fine, non-vertisol; Medium-coarse; Fine-coarse; Fine-medium; Fine-medium-coarse; Organic Fine, vertisol o o All soils are 100 cm deep and consist of two layers: 0-50 cm and 50-100 cm.
Crust storage	1-5		
Soil storage	24-109		
Scale depth (Parameter to calculate soil water storage as a function of texture	5,10,15,20,30		
Initial surface storage	0, 5, 10		
Surface roughness reduction per month	0, 50		
Maximum Rooting depth (cm)	5,30,50,100		
All soil parameters are derived from the Soil Geographical Database of Europe through a set of pedotransfer rules. Effective soil water storage capacity (SWAP) in 0-30 and 30-100cm soil layers			
Standard deviation of elevation in a 1.5km radius, derived from GTOPO30 DEM.	0-641m	Map of relief classes indicating where crop production is not possible due to steep slopes.	Map of relief classes indicating where crop production is not possible due to steep slopes.

Table 11
Land cover and land use comparison

Land cover representation / variables

PESERA inputs	*Closest Alternative from IMAGE inputs / outputs*	*Closest Alternative from LPJ / LPJmL inputs / outputs*
Land cover type/management option (see below)	Land cover type and crop type (see below)	Plant functional type, crop functional type (see below)
Surface roughness reduction per month by vegetation (0, 50 %)		
Rooting depth (5, 30, 50 or 100 mm)		
Cover (%)		
Planting and harvesting month of dominant and secondary crop (Jan-Dec)		
Water use efficiency		

Main land cover types

PESERA inputs	*Closest Alternative from IMAGE inputs / outputs*	*Closest Alternative from LPJ / LPJmL inputs / outputs*
Artificial land		
Arable land	Agriculture	
Vineyards		
Fruit trees and berry plantations		
Olive groves		
Pastures and grassland	Extensive Grassland Grassland / steppe	
Heterogeneous agricultural land		
Forest	Plantations, Regrowth forest (abandoning), Regrowth forest (timber), Biofuel, Boreal forest, Cool conifer forest, Temperate mixed forest, Temperate deciduous forest, Warm mixed forest, Tropical Forest	Tropical broadleaved evergreen, Tropical broadleaved raingreen, Temperate needle-leaved evergreen, Temperate broadleaved evergreen, Temperate broadleaved Summergreen, Boreal needle-leaved Evergreen, Boreal needle-leaved Summergreen, Boreal broad-leaved Summergreen,
Scrubs	Tundra, Scrubland, Savanna, Tropical Woodland, Wooded Tundra	Temperate herbaceous, Tropical herbaceous
Bare land	Hot desert, Ice	
Degraded natural land		
Water surfaces and wetland		

Crops / CFT's

PESERA inputs	*Closest Alternative from IMAGE inputs / outputs*	*Closest Alternative from LPJ / LPJmL inputs / outputs*
Spring cereals	Temperate cereals	Temperate cereals
Winter cereals	Tropical cereals	Tropical cereals
Maize	Maize	Maize
Root crops	Root and tuber crops	Temperate roots
Oil seeds	Oil crops	Sunflower, Rapeseeds
Forage		
Fallow		
	Rice	Rice
Pulses	Pulses	Pulses Tropical roots

Spatial distribution of vegetation

PESERA can be run using actual land cover data or simulate crop growth. The actual land cover data can be replaced by land cover simulations by IMAGE or LPJ. IMAGE and LPJ simulate spatial distribution of vegetation and crops at a 0.5° resolution. Outputs provided are dominant land cover in each grid cell (Upper part of Table 11), and fractional cover of 19 agricultural crops in agricultural land (Lower part of Table 11). Land cover and land use classifications differ between PESERA and IMAGE and LPJ, because of the difference in focus of the models and differences in the spatial extent of the model. Technically speaking, land use and land cover types from IMAGE or LPJ can however be translated into forest, grassland or scrubs as used in PESERA (Table 11). For all land use and land cover types used as input in PESERA, crop-specific parameters are set (Table 11). Several vegetation or crop types simulated in IMAGE and LPJ are not parameterized in PESERA because they either do not occur in Europe, or were not relevant for the goals of PESERA (degrading areas in Europe, focusing on agricultural land). Consequently, natural land cover types are subdivided in some broad classes that are probably not representative for the variation of vegetation at global scale. Thereby, the parameterization of crops in PESERA is specific to European conditions that often will not apply outside Europe. Several new crops thus need to be specified, parameterized and calibrated when upon using PESERA at global scale.

Finally, the models differ in how land use in agricultural land is represented. PESERA uses a dominant and secondary crop while IMAGE uses cover percentages for 19 crops. These can be translated into dominant and secondary crops, but this should be done carefully, especially with cells with a large variety of crop types.

5.3 Simulating erosion impact on crop production using IMAGE/LPJ

Spatial allocation of agriculture and the production of crops is strongly dependent on soil characteristics, including water holding capacity and fertility of the topsoil. These factors are influenced by erosion but are currently considered in IMAGE using a static input map. Theoretically, feedbacks between erosion and crop production could be included in the IMAGE framework (Figure 25).

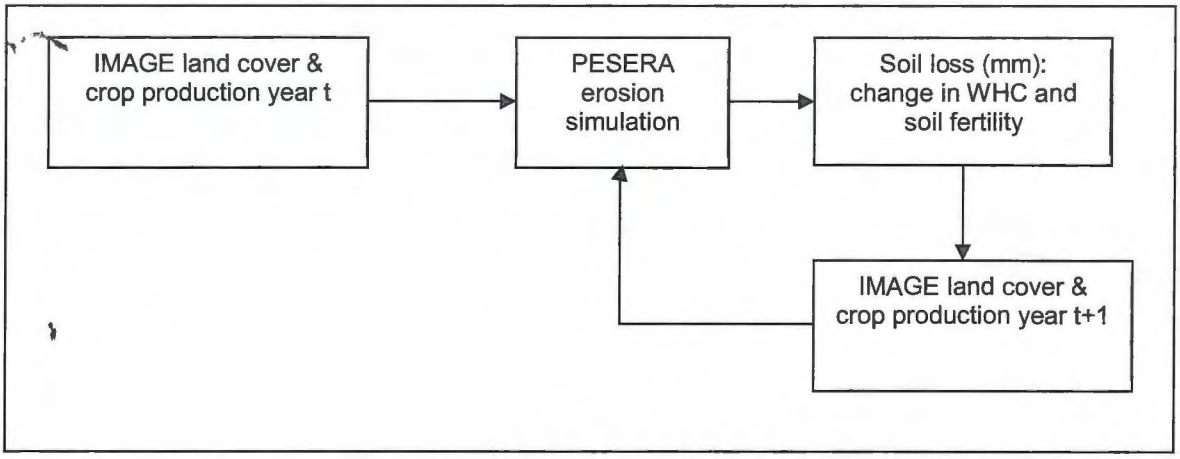

Figure 25

Potential linkage IMAGE with PESERA.

This poses two conceptual problems. First, PESERA is not a dynamic model, but simulates long-term average erosion risk under continuous vegetation and climate over 50 years. This cannot be interpreted as actual erosion rates under changing vegetation. Erosion rates are not influenced by the spatial pattern of vegetation in a certain year, but vegetation is assumed to be representative for the past fifty years.

A second issue concerns data on and simulations of soil depth. PESERA simulates erosion risk in tonnes/km^2 per year. This can be translated into millimetres soil loss using data on bulk density. However, in most cases this calculation will result in a soil loss of a few millimetres. As soil depth is extremely variable in space and data on soil depth are scarce (see Chapter 6.2), uncertainties in soil depth maps at a resolution suitable for global-scale simulations (10x10 km or coarser) are large. Data on bulk density are scarce as well. Bulk density is however strongly correlated with soil texture and could be calculated from more abundant soil texture data. This however introduces an additional uncertainty in soil depth loss calculations. Consequently, soil loss in mm simulated with PESERA will generally be smaller than the uncertainties in soil depth. Presenting PESERA outputs as mm soil loss thus would give a false impression of precision of the results that is not supported by the input data and the model structure.
When running PESERA, soil depth is classified into five classes as a best apporiximationof the variation of soil depth at this scale of analysis. In the current version of PESERA, soil depth losses as could be expected annually thus cannot be captured by a PESERA input map for a simulation for a next year.

A practical consideration upon a full coupling via modelled change of the soil depth through erosion as described above, is that the allocation and production of crops in IMAGE or LPJ should be influenced by these factors. Currently, IMAGE and LPJ are unable to cope with changes in soil depth. LPJ assumes a standard soil consisting of two layers (0-50 cm and 50-100 cm) which is static in time while in IMAGE a reduction factor is applied on the potential production, that incorporates limitations by soil fertility, soil depth, drainage, salinity and acidity. This reduction factor is also static in time. For modelling full feedbacks with erosion, the model(s) should be adapted to using a soil depth that can change over time.

Alternatively, a somewhat looser link could be established (Figure 26). Such a linkage would be possible with both the PESERA model as with the USLE-derived model currently used within the IMAGE framework. Based on IMAGE simulations, erosion risk can be simulated. Subsequently, areas projected to have severe erosion risk can be excluded from crop allocation, or may be rated less suitable for allocation of crops that aggravate erosion by e.g. changing the appropriate reduction factor in IMAGE. In a next simulation year the spatial allocation of crops will then be influenced by changes erosion risk patterns. Soil processes are not explicitly simulated, only changes in the projected impact of land use allocation on erosion.

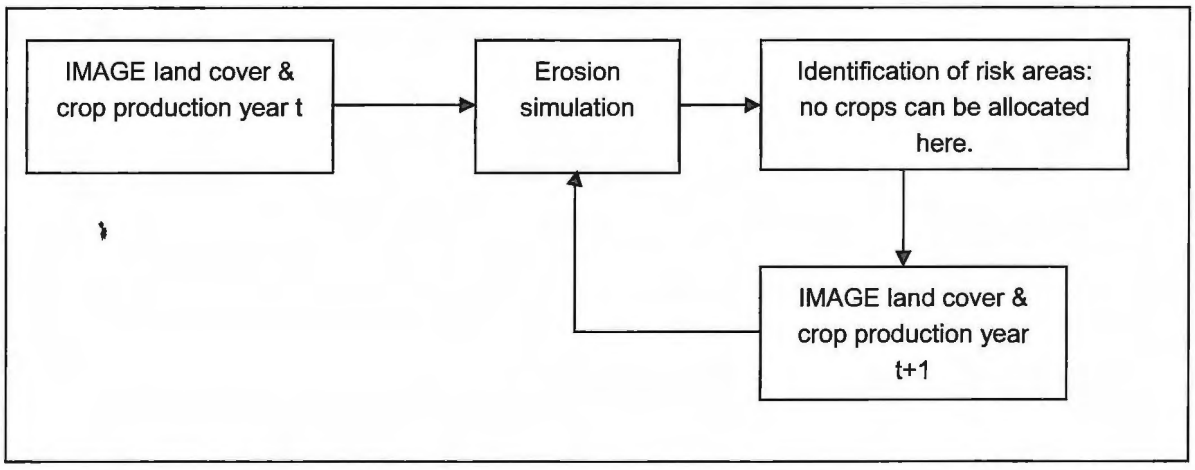

Figure 26
Possible linkage IMAGE-erosion module.

5.4 Procedure for running PESERA at global scale

5.4.1 Basis data and model adaptations

Table 12 describes basis data needed for PESERA at global scale and model adaptations that are needed for PESERA, IMAGE or LPJ.

Table 12

Data and model adaptations needed for simulating feedbacks between erosion and crop production with PESERA and IMAGE/LPJ at global scale.

1.	Create elevation dataset	Based on a global-scale DEM, derive a map of standard deviation of elevation (m) at the model run resolution. Alternatives are 90m SRTM DEM or GTOPO DEM (1km resolution). In the SRTM DEM, there are no data North of 60 degrees. GTOPO might therefore be the best alternative
2.	Create soil data set	Develop pedotransfer rules to derive – Sensitivity to crusting (5 classes) and – Erodibility (5 classes) from Harmonized World Soil Database, – Derive Effective soil water storage capacity (value range 0-250 mm); – Soil water available to plants in top 300mm (value range 0-90 mm); – Soil water available to plants (300mm and 1000mm depth, value range 0-154 mm) – depth to rock (4 classes). The Harmonized World Soil Database (HWSD) currently seems to be the best dataset for this application (see chapter 6)
4.	Create vegetation data	– Parameterize PESERA parameters for IMAGE crops rice and other crops. – Assess accuracy of PESERA natural land cover type parameterization for global scale; if necessary, parameterize natural land cover types. – Assess accuracy of PESERA crops parameterization for global scale; if necessary, parameterize crop types for global scale.
5.	Model adaptations	– Assess behaviour of PESERA outside current boundary conditions. – Adapt PESERA to run with global-scale land cover types: Add new land cover types as needed – Adapt IMAGE for running with reduction factor that can change in time, and / or – Adapt LPJ for running with map indicating unsuitable areas that can change in time. – Develop translation of PESERA erosion risk into changes of IMAGE reduction factor / suitability in LPJ.

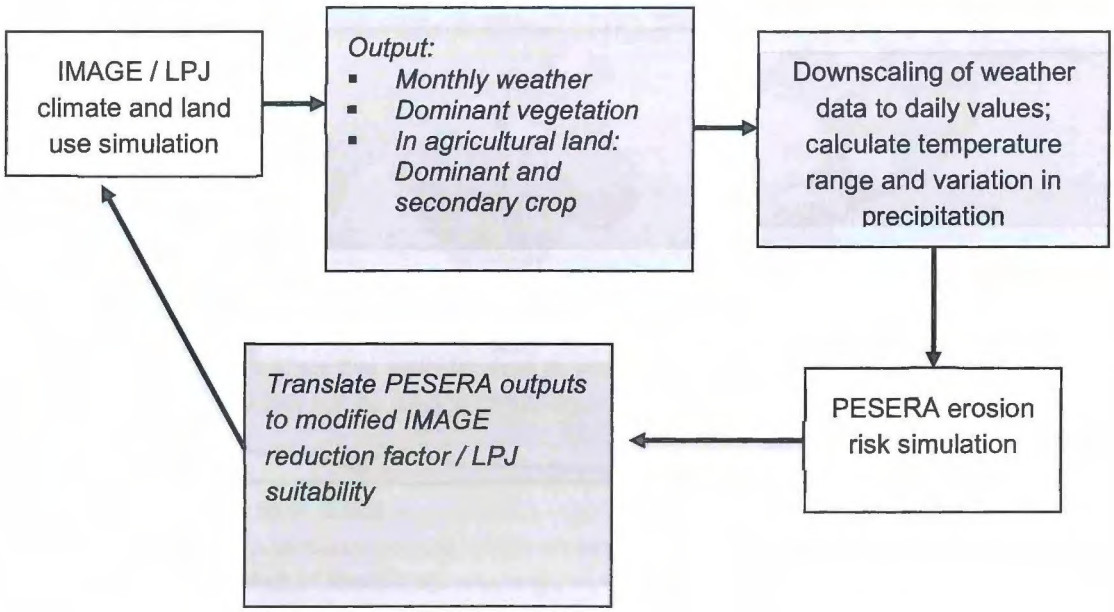

Figure 27
Technical overview of simulating feedbacks with IMAGE/LPJ and PESERA.

5.4.2 Estimate uncertainties

The PESERA regional model was developed for the European extent with a spatial resolution of 1km^2. A test for a global-scale application at 10km resolution within the European extent showed that simulation results at 10km resolution showed a reasonable match with those at 1km resolution (Table 5). Also, the 10km resolution results showed a somewhat better match with data on suspended sediment load (Table 8). The global coverage of a 1 km^2 DEM assures a topographic base line for modelling, from which coarser resolutions DEMs can be created. This will lead to added uncertainty in model outputs at global scale. Also, the regionalisation of soil and climate data will introduce much more variability and uncertainty in model output, especially in areas that have climatic, relief or land cover conditions that fall outside the model boundary conditions (Figure 28). For instance, how will the model perform for climate zones, in combination with specific terrain conditions, that are not found in Europe or in semi-arid zones? For instance, mountainous areas in the humid tropics, or the cold areas in Canada or Russia. Also in areas with low data availability, low quality data areas and on highly heterogeneous terrain (soil) conditions uncertainties in input data and uncertainty propagation in the model structure need to be considered.

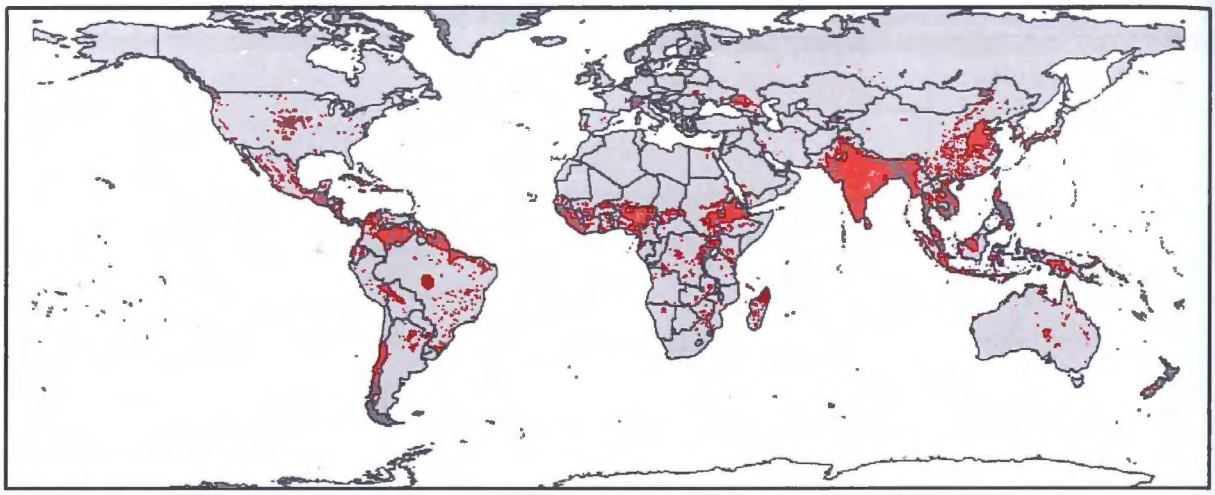

Figure 28

Areas where climatic and land cover / land use conditions are outside the PESERA boundary conditions as described in Tables 5.1-5.3. Indicated in red. Red areas in Europe indicate locations where the use of other data in IMAGE / LPJ causes exceedance of the boundary conditions.

5.5 Possibilities for improving IMAGE-USLE

As an alternative to including PESERA in the IMAGE framework, several improvements on the USLE approach currently used in IMAGE are possible.

Better parameterization of vegetation / management types: Especially in natural land cover, the parameterization is highly generalized. Based on a literature review, protection factors could be estimated for the complete range of land use and land cover types used in the GLOBIO biodiversity model. For several crops, protection factors could be adapted for each biome or different management types.
The relief index used in IMAGE-USLE is based on altitude ranges as provided by the 1:5 M scale FAO soil map of the world. In this report, we calculated the relief index based on a global-scale DEM. With the global DEMs currently available it is possible to assess if including larger elevation differences than 2% is appropriate and to assess if using an e.g. exponential, logarithmic relation between elevation differences and relief index is recommended.
In southern Europe, inaccurate patterns of IMAGE-USLE-simulated erosion risk might be explained by averaging out vegetation cover over the year. Alternatively, IMAGE-USLE could be run with a monthly time-step, so that the interactions between rain intensity and vegetation cover can be accounted for more realistically.

6 Databases for global modelling and validation

6.1 Introduction

This chapter describes maps that could be used as inputs for global-scale erosion risk simulations (section 6.2) and data that can be used to check the credibility of erosion model outputs (section 6.3).

6.2 Input soil data

FAO UNESCO Soil Map of the World
The 1:5 M scale Soil Map of the World (FAO-Unesco, 1971-1981) has long been the single harmonized global soil information resource. It was digitized in 1995 (FAO, 1995, 2003); with derived soil properties linked to the map, it has long been the most common source for global modellers.

SOTER
The SOTER project was initiated by ISRIC with support from the IUSS, FAO, and UNEP (ISSS, 1986).
The SOTER project aims to establish a World Soils and Terrain Database, at scale 1:5 000.000, containing digitized map units and their attribute data in standardized format. SOTER databases have been created at different scale levels (national SOTERs and regional/supra-national). Space Shuttle Radar Topographic Mission (SRTM) digital elevation data are now being used to derive the different landform units and to generate terrain information; soil attribute data are largely derived from legacy field data and pedotransfer functions. The present global coverage is incomplete. The program continues, but there is no structural program to support the expansion of the SOTER database for the entire world.

WISE
The ISRIC-WISE global soil profile database (Batjes, 2009) contains 10.000 geo-referenced soil profiles from 123 countries (Batjes, 1996). It has been used to derive spatial data sets of derived soil properties on a global 0.5 by 0.5 degree grid include soil pH, organic carbon content, inorganic carbon content, cation exchange capacity, and available water capacity at standard depths (0-30, 30-100, and 0-20, 20-40, 40-60, 60-80 and 80-100 cm), (Batjes, 2012). The WISE database was developed for, and has been a much used resource for, global (change) modellers.

Harmonized World Soil Database v 1.2
The HWSD was developed by the FAO's Land & Water Development Division, IIASA, ISRIC-World Soil Information, Institute of Soil Science, Chinese Academy of Sciences (ISSCAS), and the Joint Research Centre of the European Commission (JRC) (FAO/IIASA/ISRIC/ISSCAS/JRC, 2009). The database has a 30 arc-second raster resolution and contains over 15000 different soil mapping units. It is based on existing regional and national updates of soil information worldwide (SOTERs, European Soil Database, Soil Map of China, and WISE profile database) combined with the information contained within the 1:5 000 000 scale FAO-UNESCO Soil Map of the World (FAO and UNESCO 1971-1981).

The HWSD raster database is linked to a set of harmonized soil property data. These may be linked with the raster map which allows provision of information on map composition in terms of soil units and selected

soil parameters (organic Carbon, pH, water storage capacity, soil depth, cation exchange capacity of the soil and the clay fraction, total exchangeable nutrients, lime and gypsum contents, sodium exchange percentage, salinity, textural class and granulometry) (Rossiter, 2011). Maps in geotiff format are available for the single soil data properties.
Efforts are underway to upgrade the HWSD by adding available datasets to the current data source, coordinated by the FAO in the framework of the Global Soil Partnership (GSP).

Global Digital Soil Mapping Project
GlobalSoilMap.net is a global consortium that has been formed with the objective to make a new digital soil property map of the world using remote sensing and spatial statistics at fine resolution (90 m)(Sanchez *et al.*, 2009.). The aim is to compile soil property map that will be supplemented by interpretation and functionality options. The project is an initiative of the Digital Soil Mapping Working Group of the International Union of Soil Sciences IUSS. Much research work is currently done around the globe to improve standard soil maps applying spatial statistics and a range of co-variables including DEMs, climate, relief etc. Current efforts concentrate on collecting soil data and developing a soil map for the African continent. The global map will be built from regional maps and coordinated by regional nodes. A standard set of soil properties will be estimated for standardized depth intervals. In the next coming years property maps will gradually become available for countries and regions from various sources. The Global Soil Mapping Project will work towards continental and global scale coverage of soil property maps.

Conclusions
With respect to global coverage and data availability, the Harmonized World Soil Database and the FAO UNESCO soil map of the world are the two main sources for global modelling. Further, a set of WISE derived soil property maps of the world are available.

6.3 Datasets for testing and evaluation erosion risk model outputs

6.3.1 Introduction

The proposed IMAGE/LPJ-module be developed should be tested and evaluated once available. There may be two different objectives in such an exercise: 1) to verify the similarity of predictions of the IMAGE/LPJ-module with the original model, and/or to evaluate the output of the module on the basis of measured data or expert judgement.
The comparison of the predictions of the IMAGE/LPJ-module with the original model can provide a check on the adequacy of fitting the erosion model in the IMAGE/LPJ framework. The latter requires conversions and adaptations to the model and its data flows. Provided that the same data are used, the module built should provide comparable outputs.

The second objective concerns assessing the adequacy of the model for estimation of erosion and other hydraulic processes. For Europe, this has been done for the original PESERA regional model under different conditions and various scales (e.g. (Meusburger, *et al.*, 2010), (de Vente, *et al.*, 2008), (Van Rompaey *et al.*, 2003).

Evaluation of the erosion model/module should not only focus on the adequacy to estimate rate of water erosion but also on assessment of the degree to which much of the processes that affect sediment transport in the landscape are ignored, are outside the boundary conditions of the model, and what the implication is for predictions at regional to global scale. Sedimentation in the plains and valley bottoms are not taken into account and much of detached sediment is re-sedimented in another part of the landscape, while the erosion models only calculate the potential soil loss at a certain point. Mass movement of soils, such as landslides and

soil slips are processes that are not modelled by most erosion models that usually take sheet erosion only into account. For test areas in different eco-regions and landscapes an erosion assessment could be done and the known soil loss and depositional processes could then be added up and compared with the quantitative estimates of the erosion model. A difficulty is that erosion is a process of thresholds and extreme events. Slumps and landslides occur when a certain threshold is reached and significant erosion may occur only in the extreme rainfall that occur once every so many years. With the regional and global modelling the extremes in rainfall are not represented in the data. The question then is whether the predicted erosion rate is comparable with the long term average measured erosion rates.

6.3.2 Data sets for evaluation of erosion model output

WOCAT

WOCAT (World Overview of Conservation Approaches and Technologies) is a global network of Soil and Water Conservation (SWC) specialists. WOCAT makes an inventory of sustainable land management technologies and their implementation approaches providing standardized tools and methods (WOCAT, 2002).
The WOCAT database provides access to 175 case studies on technologies (the activities implemented in the field) and 130 approaches (the enabling environment required to implement the technologies successfully), as well as geographic data. The technologies database provides information on land management technologies and their effectiveness in conservation and/or enhancing productivity. For the purpose of evaluation of the erosion model, the WOCAT mapping database seems most appropriate. The case studies from the WOCAT technologies data base will be relevant for the definition of soil and land management scenarios and conservation strategies and their effect on soil erosion potential.

The WOCAT mapping database contains spatial assessments of degradation and conservation with qualitative indications of impacts on ecosystem services, including agricultural production, organic matter, and water availability. The degradation and conservation mapping ranges between local to regional. In the mapping approach the basic mapping unit is the land use system (LUS) rather than the landscape or land units. Output maps of the erosion model may be compared with the WOCAT land degradation status maps.

DESIRE

The DESIRE project has mapped various areas with the WOCAT methodology (Schwilch *et al.*, 2012). In the DESIRE project local level mapping has been done (watershed level). Data to run the PESERA model have been gathered for several of the DESIRE study sites. The data and the modelling results from some of these sites may therefore be relevant for the evaluation of the erosion proposed model/module for LPJ-IMAGE. The areas, however, are rather small (sub-watersheds).

LADA

The LADA (ref) projects has also mapped various areas with the WOCAT methodology and the GLADA methodology. In the LADA project the focus is mainly on the regional and national scale. The national degradation maps may be relevant for evaluation of the proposed model/module for LPJ-IMAGE.

USLE test plot database

The Universal Soil Loss Equation (USLE) was developed from experimental data gathered from plots across the USA. In the 1950's the USDA-ARS National Runoff and Soil Loss Data Center was created at Purdue University. It became the central location for the soil erosion data that had been collected across the U.S. since the 1930s. The Center compiled a wide range of experimental data from across the U.S, and analysed the data for further development of erosion prediction equations. A substantial database of the measured runoff and soil loss data was eventually created from 47 research stations in 24 of the 37 states east of the Rocky Mountains as well as Pullman, Washington and Mayaguez, Puerto Rico, totalling over 10,000 plot years

(Flanagan, 2004). This database is a valuable resource to date for the evaluation and validation of erosion prediction models.

Evaluation of PESERA at the catchment scale

In the framework of the DESIRE project work is being done to calibrate/validate/evaluate PESERA. For the purpose a database was developed with sediment export rates from river catchments in Europe, the Mediterranean World and the regions of the DESIRE study site areas outside Europe. This sediment yield (SY) database will allow the calibration and validation of the (adapted) PESERA model and will provide a framework to evaluate mitigation strategies at the catchment scale, considering their effects on total sediment export. The established sediment export database facilitates the comparison of erosion rates, predicted by the PESERA model, with actual sediment export rates. This comparison will serve as a basis indication where other sediment sources may be important and where additional attention needs to be given to the PESERA model. Results will be presented in a report and in articles (Vanmaercke, *et al.*, 2011).

7 Conclusions and discussion

The Study

The modified version of the USLE already available in IMAGE and PESERA were evaluated against several sources of land degradation and erosion; GLASOD, GLADA and TSS. Although this is problematic, as each of the other regional/global datasets on soil erosion has its own boundary conditions, assumptions and limitations, the comparison with various sources, provided general information on the performance of the models. Also, a study was made on the effect of DEM compilation method on model output and of DEM resolution (1 km versus 10 km) on model output.

What we found

Approaches currently used for simulating erosion risk at national scale or larger, include models based on the USLE (or similar equations such as SLEMSA), factor scoring methods, regression models and the PESERA erosion risk model. Based on literature analysis, out of this set of approaches, PESERA was evaluated as most suitable for improving erosion estimates within the IMAGE framework, because (1) the range of processes considered in PESERA better reflect the actual hydro-ecological processes that influence erosion; (2) the output of PESERA is calculated per monthly time-step and with various output variables, other than just soil loss, thus allowing for multiple linkages and interactions with the IMAGE model and providing opportunities for inputs to scenario analyses; and (3) additional data requirements to run PESERA with IMAGE are very limited because most input variables for PESERA are already used in IMAGE/LPJ. From the literature analysis, no convincing evidence was found, however, that any of the models investigated provides a more accurate reflection of water erosion for all conditions (the adequacy of models varied differently for geographic zones).

IMAGE-USLE and PESERA results for 1km and 10km resolution of the DEM for Pan-Europe, indicate that: Both IMAGE-USLE and PESERA predictions at coarser resolution (10 km) are consistent with those produced at 1 km resolution. This contradicts the claim made in several studies that PESERA will perform better on higher resolution DEM, than at lower resolution (10 km in our study).

The resampling method and the averaging process when converting between scales appear to have more impact on projections than the coarser resolution of the DEM.

Patterns of erosion risk simulated with IMAGE-USLE are not consistent with those simulated with PESERA. Although patterns of erosion risk simulated with IMAGE-USLE are more consistent with patterns of other sources for regional and global prediction of degradation/erosion, the correlations are weak. Spatial patterns of erosion risk simulated with both IMAGE-USLE and PESERA show some overlap with observed patterns of suspended sediment load in Europe.

This study cannot give a firm conclusion on the reliability of predictions of the regional erosion models studied. The data required for that are not available. We did test the models on their sensitivity in output when different resolution data (topography) were used.

The PESERA model considers a larger number of variables and processes, such as vegetation growth and hydrological processes, that are also considered in the IMAGE model.

The more process-based approach of PESERA and the more varied outputs, specified in monthly time steps, such as surface run-off, soil moisture deficit and soil erosion, and the improved availability of base line data, such as for topography, would favour the choice for PESERA as the model towards quantification of soil erosion scenarios in the IMAGE-LPJ modelling framework. There is need for a continued effort in the further application, development and testing of the PESERA model and a possible link with the IMAGE-LPJ framework. This provides opportunities for continued evaluation of the model and establishing links with the development team (University of Leeds).

8 Recommendations

Based on the results and discussion presented above, we recommend PESERA for the quantification of soil erosion in the IMAGE-LPJ modelling framework.

Technical adaptations needed for linkage of PESERA with the IMAGE framework include:
- Enabling IMAGE/LPJ to run with soil inputs that can change in time;
- Parameterization of equations that describe the effects of different type of vegetation at a global scale;
- Creation of global-scale soil and relief data layers as inputs for PESERA application
- Applying a monthly time-step
- Introduction of more detailed parameterization of protection against erosion by vegetation.

Scenario development in the global modeling framework for projections of impacts of conservation and erosion could include semi-quantitative indicators of erosion risk in feedback with crop-growth models. One way could be the methodology as was developed and tested for national level studies by Mantel, et al. (1997, 1999, 2000) in which simulated erosion over decades are translated into classes of topsoil lost, soil parameters are then adjusted for this loss. For this, the similar, but simpler, model adaptations are needed as described above. Simulating such feedbacks are possible with both IMAGE-USLE and PESERA.

Acknowledgements

This report draws on fruitful discussions with numerous colleagues. The Global Soil Information Facilities (GSIF) are being developed and implemented by a dedicated group at ISRIC in close collaboration with a growing international network of experts.

References

Albaladejo Montoro, J., Stocking, M., 1989. Comparative evaluation of two models in predicting storm soil loss from erosion plots in semi-arid Spain. CATENA 16, 227-236.

Bai, Z.G., Dent, D.L., Olsson, L., Schaepman, M.E., 2008. Global Assessment of Land Degradation and Improvement. 1 Identification by remote sensing. Report 2008/01 (GLADA Report 5), ISRIC – World Soil Information Wageningen.

Batjes NH 1996. Global assessment of land vulnerability to water erosion on a ½ by ½ degree grid. Land Degradation & Development 7, 353-365

Batjes NH 2005. ISRIC-WISE global data set of derived soil properties on a 0.5 by 0.5 degree grid (ver. 3.0). Report 2005/08, ISRIC - World Soil Information, Wageningen

Batjes, N. H. (2009). "Harmonized soil profile data for applications at global and continental scales: updates to the WISE database." Soil Use and Management 25: 124-127.

Batjes NH 2012. ISRIC-WISE derived soil properties on a 5 by 5 arc-minutes global grid (ver. 1.2). Report 2012/01, ISRIC - World Soil Information, Wageningen

Beusen, A.H.W., Dekkers, A.L.M., Bouwman, A.F., Ludwig, W., Harrison, J., 2005. Estimation of global river transport of sediments and associated particulate C, N, and P. Global Biogeochem. Cycles 19, GB4S05.

Beven KJ and Kirkby MJ 1979. A Physically Based, Variable Contributing Area Model of Basin Hydrology. Hydrological Sciences Bulletin 24 (1), 43-69

Bouwman, A.F., Kram, T., Klein Goldewijk, K., 2006. Integrated modelling of global environmental change. An overview of IMAGE 2.4. Netherlands Environmental Assessment Agency, Bilthoven.

Chakela, Q., Stocking, M., 1988. An Improved Methodology for Erosion Hazard Mapping Part II: Application to Lesotho. Geografiska Annaler. Series A, Physical Geography 70, 181-189.

Claessens, L., G. B. M. Heuvelink, et al. (2005). "DEM resolution effects on shallow landslide hazard and soil redistribution modelling." Earth Surface Processes and Landforms 30: 461-477.

Dana Tomlin C 1990. Geographic Information Systems and Cartographic Modelling Prentice Hall, Eaglesfield Cliffs, NJ, 572 p

De Roo, APJ, Wesseling, CG. and Ritsema, CJ, 1996a, LISEM: a single event physically-based hydrologic and soil erosion model for drainage basins. I: Theory, input and output: Hydrol. Proc., 10: 1107-1117.

de Vente, J., Poesen, J., Verstraeten, G., Van Rompaey, A., Govers, G., 2008. Spatially distributed modelling of soil erosion and sediment yield at regional scales in Spain. Global and Planetary Change 60, 393-415.

EEA, 1998. Europe's environment: the second assessment. European Environment Agency, EEA, Copenhagen.

Eickhout, B., Prins, A.G., Balkema, A., Bakker, M., Banse, M., den Boer, A., Bouwman, L., Elbersen, B., Geijzendorffer, I., van den Heiligenberg, H., Hellmann, F., Hoek, S., van Meijl, H., Neumann, K., Overmars, K.P., Rienks, W., Schulp, C.J.E., Staritsky, I., Tabeau, A., Velthof, G., Verburg, P.H., Vullings, W., Westhoek, H., Woltjer, G., 2008. Eururalis 2.0 Technical background and indicator documentation. Wageningen UR and Netherlands Environmental Assessment Agency, Wageningen, Bilthoven.

Elwell, H. A., 1990. The development, calibration and field testing of a soil loss and runoff model derived from a small-scale physical simulation of the erosion environment on arable land in Zimbabwe, Journal of Soil Science 41: 239-253.

FAO (1995, 2003). The Digitized Soil Map of the World and Derived Soil Properties (version 3.5) FAO Land and Water Digital Media Series 1. Rome.

FAO and UNESCO, 1971-1981. The Soil Map of the World, 1:5 M. Volumes 1 to 10. Paris, United Nations Educational, Scientific, and Cultural Organization.

FAO/IIASA/ISRIC/ISSCAS/JRC, 2012. Harmonized World Soil Database (version 1.2). FAO, Rome, Italy and IIASA, Laxenburg, Austria.

Flanagan, D., 2004. Pedotransfer functions for soil erosion models. Developments in Soil Science. Y. Pachepsky and W. J. Rawls, Elsevier. Volume 30: 177-193.

Fleskens, L., M. Kirkby, Irvine, B.J. (submitted). "The PESERADESMICE modelling framework for grid-based assessment of the physical impact and economic viability of land degradation mitigation technologies." Environmental Management DESIRE special issue.

Freedman VL, Lopes VL and Hernandez M, 1998. Parameter identifiability for catchment-scale erosion modelling: a comparison of optimization algorithms. Journal of Hydrology 207, 83-97

Geraedts, L., Recatala-Boix, L., Ano-Vidal, C., Ritsema, C.J., 2008. Risk assessment methods of soil erosion by water:: a review and recommendations. In: Risk Assessment Methods for Soil Threats. pp. 61.

Gilley, J. E., L. J. Lane, J. M. Laflen, H. D. Nicks and W. J. Rawls. 1988. USDA-water erosion prediction project: New generation erosion prediction technology. In: Modeling, Agricultural, Forest, and Rangeland Hydrology. Symposium Proceedings. Pub. 07-88:260-263. Available from Am. Soc. Agric. Eng., St. Joseph, MI.

Grohs, F. and H. A. Elwell, 1993. Estimating sheetwash erosion from cropland in the Communal Lands of Zimbabwe. Zimbabwe Science News 27.

Hootsmans R, Bouwman AF, Leemans R and Kreileman E, 2001. Modelling land degradation in IMAGE 2. RIVM Report 481508009, RIVM, Bilthoven

Hootsmans, R.M., Bouwman, A.F., Leemans, R., Kreileman, G.J.J., 2001. Modelling land degradation in IMAGE 2. In: National Institute for Public Health and the Environment, Bilthoven, pp. 33.

ISSS, 1986. Proceedings of an International Workshop on the Structure of a Digital International Soil Resources Map annex Data Base. M.F. Baumgardner, L.R. Oldeman (Eds.), ISRIC, Wageningen, pp. 138.

Kirkby, M., B. Irvine, et al., 2003. PESERA (Pan-European Soil Erosion Assessment). Third Annual Report for period 1 April '02 - 30th April '03, Work Package 1. Leeds, University of Leeds: 20 (+ appendices).

Kirkby, M.J., Irvine, B.J., Jones, R.J.A., Govers, G., Boer, M., Cerdan, O., Daroussin, J., Gobin, A., Grimm, M., Le Bissonnais, Y., Kosmas, C., Mantel, S., Puigdefabregas, J. Van Lynden, G., 2008. The PESERA coarse scale erosion model for Europe. I. Model rationale and implementation. European Journal of Soil Science 59, 1293-1306.

Kirkby, M.J., Jones, R.J.A., Irvine, B., Gobin, A., Govers, G., Cerdan, O., van Rompaey, A.J.J., Le Bissonais, Y., Daroussin, J., King, D., Montanarella, L., Grimm, M., Vieillefont, V., Puigdefabregas, J., Boer, M., Kosmas, C., Yassoglou, N., Tsara, M., Mantel, S., van der Lynden, G.W.J., Huting, J., 2004. Pan-European Soil Erosion Risk Assessment: The PESERA map version 1, October 2003. In: JRC, Ispra, Italy, pp. 30.

Klijn, J.A., Vullings, L.A.E., Van den Berg, M., Van Meijl, H., Van Lammeren, R., Van Rheenen, T., Veldkamp, A., Verburg, P.H., Westhoek, H.J., Eickhout, B., 2005. The EURURALIS study: Technical document, Report 1196. Alterra, Wageningen.

Kowal, J. M. and A. H. Kassam (1976). "Energy load and instantaneous intensity of rainstorms at Samaru, northern Nigeria." Tropical Agriculture 53: 185-197.

Lal, R. (1982). "Temperature profile of soil during infiltration." Nigerian Journal of Soil Science 2: 87-100.

Le Bissonnais, Y., Montier, C., Jamagne, M., Daroussin, J., King, D., 2002. Mapping erosion risk for cultivated soil in France. CATENA 46, 207-220.

Licciardello, F., Govers, G., Cerdan, O., Kirkby, M.J., Vacca, A., Kwaad, F.J.P.M., 2009. Evaluation of the PESERA model in two contrasting environments. Earth Surface Processes and Landforms 34, 629-640.

Lu, H., Gallant, J., Prosser, I.P., Moran, C., Priestley, G., 2001. Prediction of sheet and rill erosion over the Australian continent, incorporating monthly soil loss distribution. In: CSIRO (Ed.), CSIRO Land and Water, Canberra, pp. 40.

Loague, K.M., 1982. A comparison of techniques used in rainfall-runoff models: model efficiency The University of British Columbia, Vancouver, Canada, 258 pp.

Loague, K.M., Freeze, R.A., 1985. A Comparison of Rainfall-Runoff Modeling Techniques on Small Upland Catchments. Water Resour. Res. 21(2), 229-248.

Mantel S and van Engelen VWP, 1997. The impact of land degradation on food productivity, case studies of Uruguay, Argentina and Kenya. Report 97/01, ISRIC, Wageningen

Mantel S and Van Engelen VWP, 1999. Assessment of the impact of water erosion on productivity of maize in Kenya: An integrated modelling approach. Land Degradation and Development, 10: 577-592.

Mantel S, Van Engelen VWP, Molfino JH and Resink JW, 2000. Exploring biophysical potential and sustainability of wheat cultivation in Uruguay at the national level. Soil Use and Management, 16: 270-278.

Marx, J., 1988. Die Erodierbarkeit charakteristischer Böden im Südosten der VR China. Osteuropastudien der Hochschulen des Landes Hessen, Reihe I; Gießener Abhandlungen zur Agrar- und Wirtschaftforschung des europäischen Ostens, Bd. 162. Duncker & Humblot, Berlin, 1988; 156p.

Meusburger K, Konz N, Schaub M and Alewell C, 2010. Soil erosion modelled with USLE and PESERA using QuickBird derived vegetation parameters in an alpine catchment. International Journal of Applied Earth Observation and Geoinformation 12, 208-215

Millennium Ecosystem Assessment, 2005. Ecosystems and Human Well-being: General Synthesis. World Resources Institute, Washington, DC.

Nash, J.E., Sutcliffe, J.V., 1970. River flow forecasting through conceptual models part I - A discussion of principles. Journal of Hydrology 10(3), 282-290.

Oldeman LR, Hakkeling RTA, Sombroek WG, 1991. World map of the status of human-induced soil degradation, an explanatory note. Wageningen: International Soil Reference and Information Centre, Nairobi. United Nations Environment Programme.

Pham, T.N., Yang, D., Kanae, S., Oki, T., Musiake, K., 2001. Application of RUSLE model on global soil erosion estimate. Annual Journal of Hydraulic Engineering 45, 811-816.

Rossiter, D. G., 2011. "A Compendium of On-Line Soil Survey Information: Soil Classification for Soil Survey." from http://www.itc.nl/~rossiter/research/rsrch_ss_class.html.

Sanchez, P.A., Ahamed, S., Carr, F., Hartemink, A.E., Hempel, J., Huising, J., Lagacherie, P., McBratney, A.B., McKenzie, N.J., Mendon, M.D.L., et al., 2009. Digital soil map of the world. Science 325, 680-681.Sitch S, Smith B, Prentice IC, Arneth A, Bondeau A, Cramer W, Kaplan JO, Levis S, Lucht W, Sykes MT, Thonicke K and Venevsky S, 2003. Evaluation of ecosystem dynamics, plant geography and terrestrial carbon cycling in the LPJ dynamic global vegetation model. Global Change Biology, 2: 161-185.

Schoorl, J.M., Veldkamp, A., and Bouma, J., 2002, Modelling water and soil redistribution in a dynamic landscape context: Soil.Sci.Soc.Am.J., v. 66, p. 1610-1619.

Sonneveld, B.G.J.S., Nearing, M.A., 2003. A nonparametric/parametric analysis of the Universal Soil Loss Equation. CATENA 52, 9-21.

Stocking, M., Chakela, Q., Elwell, H., 1988. An Improved Methodology for Erosion Hazard Mapping Part I: The Technique. Geografiska Annaler. Series A, Physical Geography 70, 169-180.

Stocking, M. A. and H. A. Elwell, 1973a. Prediction of subtropical storm losses from field plot studies. Agric. Meteorol. 12: 193-201.

Stocking, M. A. and H. A. Elwell, 1973b. Soil erosion hazard in Rhodesia. Rhod. Agric. J. 70(4): 93-101.

Schwilch, G., R. Hessel, Verzandvoort, S.J.E., 2012. "Desire for greener land : options for sustainable land management in drylands."

Syvitski, J.P.M., Peckham, S.D., Hilberman, R., Mulder, T., 2003. Predicting the terrestrial flux of sediment to the global ocean: a planetary perspective. Sedimentary Geology 162, 5-24.

TEEB, 2008. The Economics of Ecosystems and Biodiversity: An Interim Report. http://ec.europa.eu/environment/nature/biodiversity/economics/pdf/teeb_report.pdf

Tomlin, C. D., 1990. Geographic Information Systems and Cartographic Modeling. Englewood Cliffs, N.J., Prentice Hall.

Tsara, M., Kosmas, C., Kirkby, M.J., Kosma, D., Yassoglou, N., 2005. An evaluation of the pesera soil erosion model and its application to a case study in Zakynthos, Greece. Soil Use and Management 21(4), 377-385.

van den Berg, M. and P. Tempel, 1995. SWEAP, a computer program for water erosion assessment applied to SOTER. Documentation version 1.5. Wageningen, ISSS.

van Engelen, V.W.P., Wen, T.T., 1995. Global and National Soils and Terrain Digital Databases (SOTER), Procedures Manual (revised edition), FAO, ISSS, ISRIC, Wageningen.

van Engelen VWP, Mantel S, Dijkshoorn JA and Huting JRM, 2004. The impact of desertification on food security in Southern Africa: A case study in Zimbabwe. Report 2004/02, ISRIC - World Soil Information, UNEP, Wageningen.

Vanmaercke, M., J. Poesen, et al., 2011. "Sediment yield as a desertification risk indicator." Science of The Total Environment 409(9): 1715-1725.

Van Rompaey AJJ, Vieillefont V, Jones RJA, Montanarella L, Verstraeten G, Bazzoffi P, Dostal T, Krasa J, de Vente J and Poesen J, 2003. Validation of soil erosion estimates at European scale. European Soil Bureau Research Report No.13, EUR 20827 EN, Office for Official Publications of the European Communities, Luxembourg.

Winiger H and Critchley W (Editors), 2007. Where the land is greener. Case studies and analysis of soil and water conservation initiatives worldwide. World Overview of Conservation Approaches and Technologies (WOCAT), Berne, Switzerland.

Wischmeyer, W.H., Smith, D.D., 1978. Predicting rainfall erosion losses - a guide to conservation planning.

WOCAT. (2002). World Overview of Conservation Approaches and technologies. 2003, from www.wocat.net.

Zhang X, Drake N, Wainwright J and Mulligan M 1999. Comparison of slope estimates from low resolution DEMS: scaling issues and a fractal method for their solution. Earth Surface Processes and Landforms, 763-779.

Appendix 1 **RUNNING PESERA MODEL**

Resolution 1km used as the base grids

Results_10kmDEM_res1km:
All the grids used with 1km resolution, but only std_eudem2 10 km grid resampled to 1km resolution (bilinear)

---

std_eudem2 (10km grid) was made with bilinear resampling from SRTM 4.1

Input file for running Pesera model:
FTN_INPUT.DAT: 1 km grids

2724	Number of rows in the analysis window
3199	Number of columns in the analysis window
0.000000E+00	Predicted change in rainfall intensity
1000.0	Grid resolution (m)
-1594713	Lower left x-ordinate
-1312168	Lower left y-ordinate
2	lu_scenario; 2=eu12crop1
1	climatescenario

In directory d:\Meteo_grids 1km

cov_jan – cov_dec	newrf1301 – newrf13012	newtemp1 – newtemp12
swsc_eff_2		
crust_0702	mtmean1 – mtmean12	itill_m
use		
cvrf21 –cvrf212	mtrange1 – mtrange12	p1xswap1
zm		
erod_0702	eu12crop1	p2xswap2
meanpet301 – meanpet3012	eu12crop2	rootdepth
meanrf1301 – meanrf13012	cvrf21 – cvrf212	rough0
meanrf21 – meanrf212	itill_crop1	rough_red
mtmean1 – mtmean12	itill_crop2	std_eudem2

Running the model

The base files for running model in d:\temp_ascii

ArcInfo Grid:
&workspace d:\meteo_grids
&run d:\temp_ascii\xgridascii083.aml
xxxxxxxxxxxxxxxxxxxxxxxxxxxxxxxxxxxxxxxxxxxxxxxxx
ftn_input083.exe (Look for input: ***FTN_INPUT.DAT)***
ftn_combined_083.exe
pesera_grid103.exe
to_grid083b.exe
xxxxxxxxxxxxxxxxxxxxxxxxxxxxxxxxxxxxxxxxxxxxxxxxx

ArcInfo Grid:
&workspace d:\temp_ascii
&run xasciigrid083.aml

Resampling 1 km to 10km

sedi_tot 1km run resampled to 10km using raster calculator:
sedi_tot_1km * 1 with processing extent of sedi_tot_10km; Snap Raster: sedi_tot_10km; Raster analysis: cell size
same as sedi_tot_10km and mask of sedi_tot_10km

Creating point file

1. sedi_tot_1km_resampled to 10km: Conversion -> raster to point
2. sedi_tot_1km(1okm DEM) to 10km: Conversion -> raster to point

Intersecting point files

These shapefiles: Analysis Tools -> Overlay -> Intersect
DBF file of resulting shapefile imported in excel for correlation calculation.
Results:
Overlay (Intersect) of 1 and 2 : Correlation sedi_tot_10kmDEM_res1km versus 1kmres10 (see: result_corrxxx..xlsx) = 0.45

Appendix 2 **RESAMPLING DEM DATA**

Resolution 1km used as the base grids
Resolution 10km: All the grids in d:\meteogrids resampled (bilinear) to 10 km

---

Results_10kmDEM_res1km: (not used in further analysis)
All the grids used with 1km resolution, but only std_eudem2 10 km grid resampled to 1km (nearest) resolution

---

std_eudem2 (1km grid) and std_eudem2 (10km grid) were made with bilinear resampling from SRTM 4.1

Run A: std_eudem2 10km bilinear
Run B: Same as Run A but std_eudem2 1km (DEM) grid with fishnet creating resampled to 10 km

---

Creating fishnet for the DEM:
Data Management Tools -> Feature Class -> Create Fishnet
Projection: Lambert Azimuthal Equal Area Central Meridian: 9 Latitude of Origin: 48
X-coordinate: -159713 Y-coordinate: -1312168
Y-axis coordinate
X-coordinate: -159713 Y-coordinate: 1411832
Cell Size Width: 10000
Cell Size Height: 10000
Number of rows: 272
Number of columns: 320
Geometry Type: Polygon
Result: FISHNET
Calculating Shape ID from FID -> Fieldcalculator replace ID with values of FID
Spatial Analyst Tools -> Zonal -> Zonal Statistics as Table
Input raster or feature zone data: FISHNET
Input value raster: std_eudem2 1km
Zone field: ID
Ignore NoData
Statistics: MEAN
Result: Zonal_MEAN
Join table Zonal_MEAN to FISHNET
Converse FISHNET (with join) to raster:
Conversion Tools -> To Raster -> Polygon to Raster (cell size 10000)
Result: pol_rast
Spatial Analyst Tools -> Extraction -> Extract by Mask
Input raster: pol_rast
Input raster or feature mask data: std_eudem2 1km grid
Result: pol_rast_mask
For running in PESERA model rename pol_rast_mask to std_eudem2

Input file for running Pesera model:

FTN_INPUT.DAT: 10 km grids

272	Number of rows in the analysis window
320	Number of columns in the analysis window
0.000000E+00	Predicted change in rainfall intensity
10000.0	Grid resolution (m)
-1594713	Lower left x-ordinate
-1312168	Lower left y-ordinate
2	lu_scenario; 2=eu12crop1
1	climatescenario

FTN_INPUT.DAT: 1 km grids

2724
3199
0.000000E+00
1000.0
-1594713
-1312168
2
1

In directory d:\Meteo_grids the coverages: (ALL these grids were resampled bilinear to 10km in the run for the 10km scenarios.)

cov_jan – cov_dec	newrf1301 – newrf13012	newtemp1 – newtemp12	swsc_eff_2
crust_0702	mtmean1 – mtmean12	itill_m	
use			
cvrf21 –cvrf212	mtrange1 – mtrange12	p1xswap1	
zm			
erod_0702	eu12crop1	p2xswap2	
meanpet301 – meanpet3012	eu12crop2	rootdepth	
meanrf1301 – meanrf13012	cvrf21 – cvrf212	rough0	
meanrf21 – meanrf212	itill_crop1	rough_red	
mtmean1 – mtmean12	itill_crop2	std_eudem2	This file to be replaced for Run A resp. Run B

Running the model

The base files for running model in d:\temp_ascii

ArcInfo Grid:
&workspace d:\meteo_grids
&run d:\temp_ascii\xgridascii083.aml
xxxxxxxxxxxxxxxxxxxxxxxxxxxxxxxxxxxxxxxxxxxxxxxxxx
ftn_input083.exe (Look for input: ***FTN_INPUT.DAT)***
ftn_combined_083.exe
pesera_grid103.exe
to_grid083b.exe
xxxxxxxxxxxxxxxxxxxxxxxxxxxxxxxxxxxxxxxxxxxxxxxxxx
ArcInfo Grid:
&workspace d:\temp_ascii
&run xasciigrid083.aml

Resampling 1 km to 10km

sedi_tot 1km run resampled to 10km using raster calculator:
sedi_tot_1km * 1 with processing extent of sedi_tot_10km; Snap Raster: sedi_tot_10km; Raster analysis: cell size
same as sedi_tot_10km and mask of sedi_tot_10km

Creating point files

1. sedi_tot_1km_resampled to 10km: Conversion -> raster to point
2. sedi_tot_10km bilinear: Conversion -> raster to point
3. sedi_tot_10km fishnet: Conversion -> raster to point
4. sedi_tot_1km_fishnet_resampled 10km: Conversion -> raster to point

Intersecting point files

These shapefiles: Analysis Tools -> Overlay -> Intersect
DBF file of resulting shapefile imported in excel for correlation calculation.
Results:
Overlay (Intersect) of 1 and 2: Correlation bilinear versus 1kmres10 (see: Correlations.xlsx) = 0.30
Overlay (Intersect) of 1 and 3: Correlation fishnet versus 1kmres10 (see: Correlations.xlsx) = 0.33
Overlay (Intersect) of 1 and 3: Correlation fishnet versus 1kmres10 (use resampled focalstat 3x3 majority) = 0.38
Overlay (Intersect) of 2 and 3: Correlation bilinear versus fishnet (see: Correlations.xlsx) = 0.82
Overlay (Intersect) of 3 and 4: Correlation fishnet versus 1kmres10_fishnet (see: Correlations.xlsx) = 0.57

Appendix 3 **PESERA output at two resolutions**

PESERA output at two resolutions (DEM = 1 and 10 km) in monthly means.

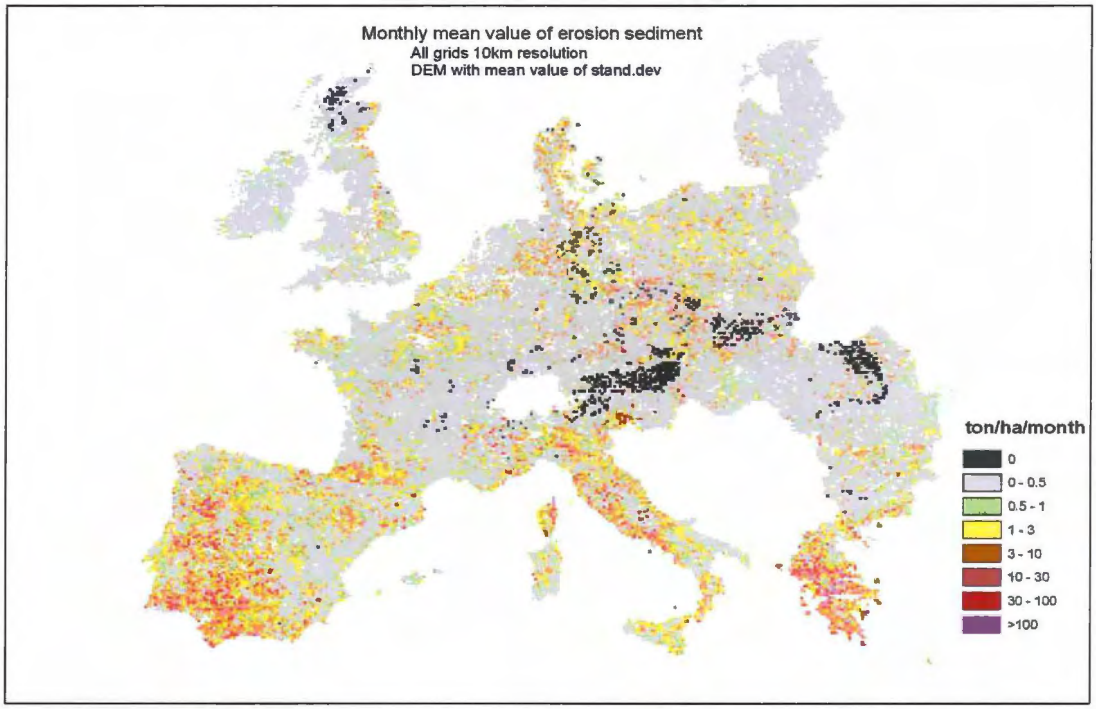

Figure 30

PESERA-estimated soil erosion (ton.ha-1.month-1), monthly mean value, based on 1 and 10 km DEM.

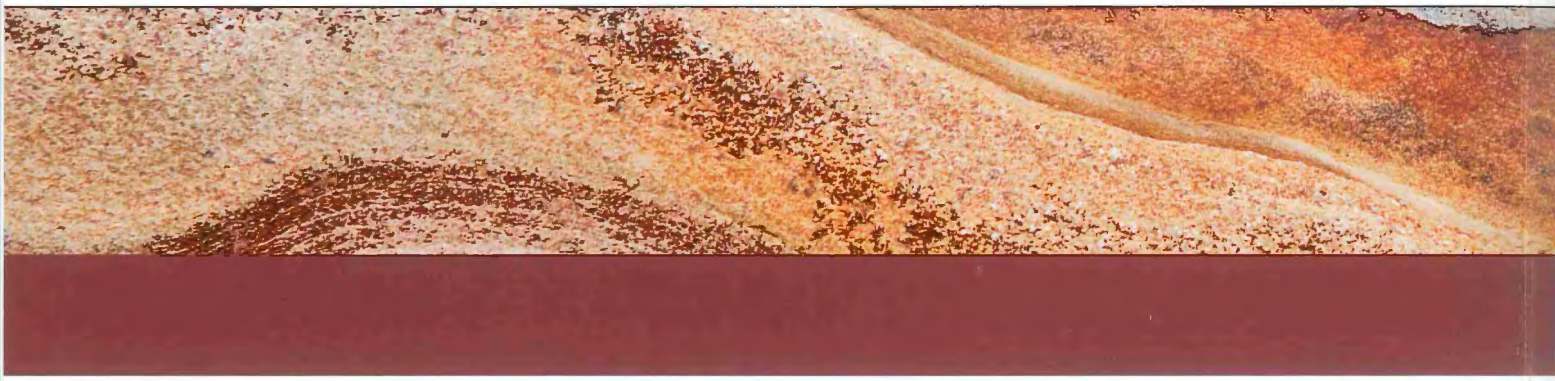

ISRIC – World Soil Information has a mandate to serve the international community as custodian of global soil information and to increase awareness and understanding of soils in major global issues.

More information: www.isric.org

WAGENINGEN UR
For quality of life

ISRIC – World soil Information has a strategic association with Wageningen UR (University & Research centre)